SINGULAR-PERTURBATION ANALYSIS OF CLIMB-CRUISE-DASH OPTIMIZATION

by

Uday J. Shankar

Thesis submitted to the Faculty of the
Virginia Polytechnic Institute and State University
in partial fulfillment of the requirements for the degree of
Master of Science
in
Aerospace Engineering

APPROVED:

E.M.Cliff, Chairman

H.J.Kelley

F.H.Lutze

May 1985

Blacksburg, Virginia

SINGULAR-PERTURBATION ANALYSIS OF CLIMB-CRUISE-DASH OPTIMIZATION

by

Uday J. Shankar

E.M.Cliff, Chairman

Aerospace Engineering

(ABSTRACT)

The method of singular-perturbation analysis is applied to the determination of range-fuel-time optimal aircraft trajectories.

The problem is shown to break down into three sub-problems which are studied separately. In particular, the inner layer containing the altitude path-angle dynamics is analyzed in detail. The outer solutions are discussed in an earlier work.

As a step forward in solving the ensuing nonlinear two-point boundary-value problem, linearization of the equations is suggested. Conditions for the stability of the linearized boundary-layer equations are discussed. Also, the question of parameter selection to fit the solution to the split boundary conditions is resolved. Generation of feedback laws for the angle-of-attack from the linear analysis is discussed.

Finally, the techniques discussed are applied to a numerical example of a missile. The linearized feedback solution

is compared to the exact solution obtained using a multiple shooting method.

To

My Parents and Sisters

And

Ms.Doris Day

ACKNOWLEDGMENTS

I am indebted to Dr.E.M.Cliff and Dr.Kelley for the help and guidance they have given me. I wish to thank Dr.F.H.Lutze for serving on my committee and for making several helpful suggestions.

I take this opportunity to thank all my friends for their help and advice.

LIST OF SYMBOLS

A ..... State matrix

B ..... Control matrix

C_D ..... Lift coefficient

C_L ..... Lift coefficient

E ..... Specific energy

g ..... Acceleration due to gravity

$H, \bar{H}$ ..... Pseudo-Hamiltonian

H^0, H^1, H^2 ..... Parts of the Hamiltonian

h ..... Altitude

J ..... Cost function

L ..... Lift

R ..... Range

t ..... Time

T ..... Thrust

V ..... Airspeed

V ..... Average airspeed

W ..... Weight, Modal matrix

W_f ..... Fuel used

x ..... State vector

SUPERSCRIPTS

$\dot{}$ ..... Time derivative

$_{0}$ ..... Stretched-time derivative

t ..... Transpose

* ..... Transpose-conjugate

GREEK SYMBOLS

α ..... Angle of attack

γ ..... Flight-path angle

δ ..... Variation

$\varepsilon^1, \varepsilon^2, \varepsilon^3$ ..... Small parameters for singular perturbation

η ..... Throttle setting

λ ..... Co-state vector

$\lambda_{()}$ ..... Co-state variable

μ ..... Weights in cost function

ν ..... Constant Lagrange multiplier

σ ..... Thrust inclination, stretched time

τ ..... Stretched time

ψ ..... End condition

TABLE OF CONTENTS

LIST OF ILLUSTRATIONS

CHAPTER 1. INTRODUCTION

Whereas there has been a considerable amount of research on time-optimal atmospheric flight trajectories, relatively little is known about such problems in the presence of fuel constraints.

The civilian applications opf fuel-optimal flight are not difficult to envisage. Fuel costs have risen rapidly over the past few years. According to Knox [12], between 1970 and 1980, the average fuel costs rose by 1000%. In 1970, fuel costs accounted for a quarter of the direct operating costs. Today this ratio is about 60-70%. Collins [7], estimates that the airlines' losses in 1980 of $286 billion could have been erased with a 3% saving on fuel. Most of the route planning used to be based on minimum time. Now there is a need to change the current planning techniques to ones with more emphasis on minimizing fuel consumption. One main feature of NASA's research today focuses on energy management [12].

In military applications, the reasons are different, but the consequences are the same. Airplane weight is a very expensive commodity in terms of costs, fuel and performance. Minimum time trajectories demand a very high operating velocity, which takes its toll on fuel consumption. For instance the F-15 aircraft can fly, fully loaded, for about 6 min. with its afterburner on. Thus a cruise-dash optimal

trajectory is imperative, if the airplane is to prove effective.

The general problem can be viewed in many ways, in terms of the cost functions and the end conditions [6]. Three of the more common are :

- Minimize a weighted sum of time and fuel with a specified range. Then the performance index is, $J = \mu_T t_f + \mu_F W_f$ with the end condition, $\psi = R(t_f) - R_f = 0$. The relative importance of fuel and time are determined by μ_F and μ_T.

- Achieve a trade-off between time and range with a specified amount of fuel. Then, $J = \mu_T t_f - \mu_R R(t_f)$ with $\psi = W_f(t_f) - W_{f0} = 0$.

- Finally, maximize the range using a specified amount of fuel and achieving a specified average speed. In this case, $J = - R(t_f)$ with $\psi_1 = W_f(t_f) - W_{f0} = 0$ and, $\psi_2 = R(t_f) - \bar{V} t_f = 0$.

Intuitively, one would expect the three problems to be equivalent. It is shown in ref [6] that while the three are closely related, they are not exactly equivalent. The three problems are Mayer reciprocals of each other.

One other aspect of the general study is the practical application. The applications are mainly in real-time and

on-board on aircraft, which severely limits the computational capacity available. One approach which suggests itself is the method of singular-perturbation analysis [9]. The application of optimal-control theory to the trajectory problem stated produces a nonlinear two-point-boundary-value-problem, with inequality constraints and an unstable system of differential equations. Singular perturbation uses the philosophy of "divide and conquer". This alleviates the problem to some extent in that the different states are dealt with separately. The reason that this can be done is that the different states may vary at different rates. Moreover, approximations in terms of simple linear feedback controls can be obtained from the analysis [14]. But, it is to be noted that the approximate feedback solutions must be well tested against exact solutions of the problem.

Another important aspect is the choice of the proper model. In ref. [3], the hierarchy of different models and their merits and demerits are discussed. With proper modeling, unnecessary complications can be avoided.

In the next chapter, a range-fuel-time optimal flight problem is formulated. The singular perturbation method is applied,and the sub-problems are discussed. The main problem looked into, the altitude-path angle dynamics is formulated in detail. In chapter three, the linearization process is discussed. Possibilities of instabilities are suggested. Conditions for the occurrences or the non-occurrences of

these instabilities are discussed. Next, these ideas are applied to a numerical example of a missile. In chapter five, feedback laws are generated for the numerical example and their performance are evaluated. Finally conclusions are drawn and the direction for further study indicated.

CHAPTER 2. FORMULATION OF THE PROBLEM

2.1: INTRODUCTION

In this chapter, a range-fuel-time optimal-trajectory-shaping problem is formulated. Some discussion is provided concerning the use of singular-perturbation theory to divide and thus, to conquer the problem. The specific sub-problem involving the 'fast' altitude path-angle dynamics is developed.

2.2: SYSTEM DYNAMICS

The dynamic model for the aircraft is based on the assumptions of vertical-plane motions. Further, the rigid-body dynamics and structural vibrations are ignored.

The state-variables selected are the altitude (h), flight-path angle (γ), specific energy (E), range (R) and the fuel-consumed (W_f). The controls include the angle-of-attack (α) and the throttle-setting (η). The system equations are :

$$\varepsilon^2 \dot{h} = V \sin\gamma$$

$$\varepsilon^2 \dot{\gamma} = \frac{g}{V} \left[\frac{L + \varepsilon^1 T \sin\alpha}{W - \varepsilon^1 Wf} - \cos\gamma \right]$$

$$\varepsilon^1 \dot{E} = V \left[\frac{T\,(1 + \varepsilon^1(\cos\alpha - 1)) - D}{W - \varepsilon^1 W_f} \right]$$

$$\dot{R} = V \cos\gamma$$

$$\dot{W}_f = Q \qquad (2.1)$$

Here, E is defined as : $E = h + V^2/2g$. and σ is the thrust inclination to the path.

In these equations, ε^1 and ε^2 are small parameters that distinguish variables having different rates, in the spirit of singular-perturbation theory. The ε^3 parameter provides a means for the standard perturbation treatment of the commonly used simplifications. With ε^3 equal to zero the equations include the assumptions of constant weight and thrust along the flight path.

As stated previously, we seek to minimize

$$J = \mu_T\, t_f - \mu_R\, R(t_f) \quad \text{with } W_f(t_f) = W_{f0} \text{ (specified)} \qquad (2.2)$$

The amount of fuel W_{f0} and the weights μ_T and μ_R are specified. The task of determining a throttle-setting history $\eta^*(t)$ and an angle-of-attack history $\alpha^*(t)$ to minimize the cost functon (2.2) for the system (2.1) is a formidable one. While modern software [5] and high-speed digital com-

puters may be successfully applied to solve it numerically for specific initial conditions, this approach is certainly not suitable for real-time on-board use.

In order to produce an implementable control, one is led to approximations. As noted above, with ε^3 set to zero, the system (2.1) is somewhat simplified. In principle, one could solve this simplified problem ($\varepsilon^3=0$) and then attempt to correct the solutions for non-zero ε^3 This is a standard perturbation problem [9]. Note, however, that setting $\varepsilon^1$and/or ε^2 to zero reduces the dynamic order of the system. This is the special character of a singular perturbation.

The use of mathematical theory of singular perturbations in flight control problem was pioneered by Kelley [9]. It has been used in a growing number of applications [1,2,3,4,8,14].

Proceeding as in [6] one seeks to employ the Maximum Principle [4,11] to characterize the optimal controls. Accordingly, one is led to define

$$H^0 = -\lambda_R V \cos\gamma + \lambda_F Q$$

$$H^1 = \lambda_E V (T-D)/W$$

$$H^2 = \lambda_h V \sin\gamma + \lambda_\gamma (g/V) (L/W - \cos\gamma) \qquad (2.3)$$

The pseudo-Hamiltonian for the problem is

$$\bar{H} = H^0 + H^1 / \varepsilon^1 + H^2 / \varepsilon^2 \qquad (2.4)$$

Following the discussion in [6], the λ's (co-states) above are actually the Lagrange multipliers for the equality constraints when the the ε's are set to zero. The multiplier on the range is taken to be $-\lambda_R$ after the fact that it is equal to $-\mu_R$ Then the the pseudo-Hamiltonian for the system, with, the assumptions made, is :

$$H = H^0 + H^1 + H^2 \tag{2.5}$$

The co-states satisfy the Euler-Lagrange equations :

$$\varepsilon^2 \dot{\lambda}_h = - \partial H / \partial h$$

$$\varepsilon^2 \dot{\lambda}_\gamma = - \partial H / \partial \gamma$$

$$\varepsilon^1 \dot{\lambda}_E = - \partial H / \partial E$$

$$\dot{\lambda}_R = + \partial H / \partial R = 0$$

$$\dot{\lambda}_F = - \partial H / \partial W_f = 0 \tag{2.6}$$

According to the Minimum-Principle [4,11], if $\eta^*(t)$, $\alpha^*(t)$ are the optimal control histories, then there is a solution to the co-state equations (2.6) such that the controls minimize the pseudo-Hamiltinian function (2.5) at all times. In addition to the differential equations (2.1) and (2.6) one

has boundary conditions on the state and co-state variables. The exact form of the conditions depend on precise specifications of initial and final state values. In general some conditions are specified at the initial points and others at the end point, so that one must solve a nonlinear two-point-boundary-value problem (NL2PBVP). For moderately complex systems, such problems are very difficult to solve. Thus, one is led to the singular-perturbation approximation. In fact, three sub-problems arise by considering the behavior of the original problem as ε^2 and/or ε^1 go to zero. In the next sections these problems are analyzed seperately.

2.3: THE OUTER OR 'CRUISE-DASH' LAYER.

The outer layer examines the behavior when both ε^1 and ε^2 go to zero. The corresponding variables (h, γ and E) are no longer state variables but are reduced to control variables. Range and fuel-weight are the only state-variables. The right-hand sides of the degraded state-variables, become equality constraints on the problem. This dictates that γ=0, L=W and T=D. For fixed h and E, the controls γ, α and η are then given by the constraints. The altitude and energy are those that minimize the H^0 part of the Hamiltonian, since, H^1 and H^2 are identically zero.

This is examined in more detail in [6]. The analysis produces the 'best' h,E combination for the cruise-dash for

the given cost function. An interesting point that comes out of the analysis is that, for some cases, the optimal altitude and energy can jump when the weights μ_T and μ_R are changed by a small amount [3].

2.4: FIRST BOUNDARY-LAYER: ENERGY TRANSITION

The 'optimal' energy as computed in the reduced problem will not generally satisfy the initial boundary conditions on E. To resolve this discrepancy (the outer solution assumes a jump) one has to consider the energy transient by examining the equations as ε^2 goes to zero. In the energy-layer, a time-stretching is introduced via $\tau=t/\varepsilon^1$. Then with τ as the independent variable, the equations are as in [6].

In the energy-layer, h and γ are still control variables as the corresponding rates are removed. Energy is the only state variable. Range and fuel-consumed do no vary in the energy-layer. As shown in [9], the cost function for the energy-layer can be identified as:

$$J = \mu_T t_f - \mu_R R(t_f) + \lim_{\tau\to\infty} \int_0^\tau H^0 \, d\tau \qquad (2.7)$$

γ and α are again obtained from the equality constraints. The analysis picks the best altitude and throttle commands (as functions of energy) as those that minimize $H^0 + H^1$ (H^2

is identically zero). Ref.[6] examines this layer in detail. There is a possibility of chattering behavior [8].

2.5: INNER-LAYER : H-γ DYNAMICS

The energy-layer dictates a command altitude and zero path-angle which may differ from the initial conditions on these states. The energy-layer assumes discontinuities in these variables. Further time scaling gives us the altitude path-angle dynamics which 'fairs' the jumps.

Defining $\sigma = \varepsilon^1 \tau/\varepsilon^2 = t/\varepsilon^2$, the system equations in terms of the new independent variable σ (with $^0 \equiv \partial(.)/\partial\sigma$) :

$$h^0 = V \sin\gamma$$

$$\gamma^0 = \frac{g}{V}\left[\frac{L}{W} - \cos\gamma\right]$$

$$E^0 = \varepsilon^1 \left[\frac{T - D}{W}\right] V$$

$$R^0 = \varepsilon^2 V \cos\gamma$$

$$W_f{}^0 = \varepsilon^2 Q \qquad (2.8)$$

The corresponding co-state system is:

$$\dot{\lambda}_h = - \partial H / \partial h$$

$$\dot{\lambda}_\gamma = - \partial H / \partial \gamma$$

$$\dot{\lambda}_E = - \varepsilon^1 \partial H / \partial E$$

$$\dot{\lambda}_R = + \varepsilon^2 \partial H / \partial R = 0$$

$$\dot{\lambda}_F = - \varepsilon^2 \partial H / \partial W_f = 0 \qquad (2.9)$$

The zeroth-order approximation to the boundary-layer is obtained by letting ε^1 and ε^2 go to zero. Then energy, range and the fuel used and their co-states are all constant. Speed is given by the relation, $V = (2g (E-h))^{1/2}$

With these conditions, the boundary-layer equations reduce to :

$$\dot{h} = V(h) \sin\gamma$$

$$\dot{\gamma} = \frac{g}{V(h)} \left[\frac{L(h,\alpha)}{W} - \cos\gamma \right]$$

$$\dot{\lambda}_h = - \frac{\partial H(h,\gamma,\alpha,\eta)}{\partial h}$$

$$\overset{\circ}{\lambda}_{\gamma} = - \frac{\partial H(h,\gamma,\alpha,\eta)}{\partial \gamma} \tag{2.10}$$

The cost function for the inner-layer is:

$$J = \mu_T \sigma_f - \mu_R R(\sigma_f) + \lim_{\sigma \to \infty} \int_o^{\sigma} (H^0 + H^1) d\sigma \tag{2.11}$$

The Hamiltonian for the h-γ dynamics is then

$$H = H^0 + H^1 + H^2 \tag{2.12}$$

The application of the minimum principle then leads to the optimal controls η and α

The throttle command is unusual in that it does not appear in the state system, but only in the Hamiltonian and hence the costate system. As prescribed by the minimum principle, η is that value that minimizes the Hamiltonian. For the problem at hand, the optimal throttle satisfies the condition,

$$(\lambda_E \, V/W) \, (\partial T/\partial \eta) - \lambda_F \, \partial Q/\partial \eta = 0 \tag{2.13}$$

If the throttle has an altitude dependent limit, then one needs to limit the throttle by an inequality condition that is a function of the state h, say, $\eta \leq \eta_{max}(h)$. In that case

the inequality constraint is adjoined to the Hamiltonian with a Lagrange multiplier, as described in [4]. In this spirit, define

$$C(h,\eta) = \eta_{max}(h) - \eta \qquad (2.14)$$

and augment the Hamiltonian with the added term $\nu C(h,\eta)$, where ν is a constant Lagrange multiplier. If the constraint is satisfied with a margin ($C>0$), then $\nu=0$ and the optimal η is a root of eqn.(2.13). If, however, the constraint is active, ($C=0$), then the optimal control is found from eqn.(2.14), with ν given by:

$$\partial H(\eta)/\partial\eta + \nu\partial C/\partial\eta = 0.$$

or

$$\nu = \partial H/\partial\eta \qquad (2.15)$$

The constraint C also provides an extra term in the λ_h° equation (eqn.2.10), viz:

$$\lambda_h^{\circ} = -\partial H(h,\gamma,\alpha,\eta)/\partial h - \nu\ \partial\eta_{max}/\partial h \qquad (2.16)$$

The optimal angle-of-attack is that which minimizes the Hamiltonian. That is, α is obtained from :

$$\partial H(h,\gamma,\alpha,\eta)/\ \partial\alpha = 0, \text{ which leads to:} \qquad (2.17)$$

$$\lambda_\gamma \; g \; C_L' \; / \; V \; - \; \lambda_E \; V \; C_D' \; = 0. \qquad (2.18)$$

where the prime indicates a derivative with respect to α.

There are two different constraints on the angle-of-attack. The first is an upper (and sometimes lower) bound on the angle-of-attack or equivalently a bound on the C_L. This constraint is similar to the one on the throttle and is treated similarly.

The second constraint on the angle-of-attack arises out of the structural load limit on the aircraft. In this case, the constraint is defined as

$$C(h,\alpha) = Q(h) \; S \; C_L(\alpha) \; - \; n_{max} \leq \; 0 \qquad (2.19)$$

where, Q and S are the dynamic pressure and the wing area respectively. This constraint is a little different in that it is a function of both the control α and the state h. This constraint can treated exactly as the earlier one by adjoining $\nu C(h,\alpha)$ to the Hamiltonian. If the constraint is satisfied with a margin, ν=0 and the α is is given by eqn.(2.20). If the constraint is active, then α is given by a zero of eqn.(2.19), with ν from:

$$\partial H(\alpha)/\partial\alpha + \nu\partial C(h,\alpha)/\partial\alpha = 0.$$

Again, the constraint adds another term to the $\dot{\lambda}_h$ equation:

$$\dot{\lambda}_h = -\partial H(h,\gamma,\alpha,\eta)/\partial h - \nu\partial C(h,\alpha)/\partial h. \qquad (2.20)$$

The boundary conditions on the problem are of the split kind. At σ=0, the altitude and path-angle are as specified in the original problem. At the final time, $h=h_c$ and γ=0, as specified by the energy-layer.

The final time is open. The other free parameters in the problem are initial values of the multipliers. Of particular interest is the singular boundary-value problem [9] where the final time is unbounded. This is of interest as we expect the state variables to reach their equilibrium values asymptotically.

The problem is then a non-linear two point boundary value problem with possible complications such as inequality constraints. The next step is to solve the equations.

2.6: TOWARDS A SOLUTION

While the adjoint equation for λ_γ is fairly simple, the equation for λ_h involves $\partial H/\partial h$ which is usually very messy. In principle, one could use the first integral, H = constant to solve for λ_h so that only the remaining three equations need be integrated. In practice, this is not trivial, since, near γ = 0, solving for λ_h leads to an indeterminate form of

the type 0/0. Moreover, this may not be very accurate numerically. So it is better to integrate the four equations, notwithstanding the complexity. Moreover this approach has a bonus in that H = constant can be used as a check on the solution.

Several methods can be used to solve the NL2PBVP. Methods like the gradient projection method have been used [1,2]. The most promising method seems to be the multiple-shooting method [5].

As suggested in [1] one can linearize the boundary layer equations in the neighborhood of the "equilibrium" value : i.e., the energy-layer solutions : $h = h_c$, $\gamma = 0$ and appropriate co-states. The linearized eigenvalues have the usual Hamiltonian structure of eigenvalues : roots are located symmetrically about the real and imaginary axes. The initial conditions on the co-states can, then, be be selected to suppress the instabilities caused by the unstable modes, so that the linearized equations produces a trajectory that will fair asymptotically into the equilibrium point. For this it is essential that the real parts of the eigenvalues be non-zero. Linearization and stability is the topic of the next chapter.

CHAPTER 3. LINEARIZATION AND STABILITY.

3.1: INTRODUCTION

As suggested in the previous chapter, it is worthwhile to investigate the behavior of the linearized boundary-layer equations.

The boundary-layer equations are linearized about the equilibrium point i.e., $h=h_c(E)$, $\gamma=0$ and "appropriate" λ_h and λ_γ. The next section explains what these "appropriate" values are.

3.2: APPROPRIATE COSTATE VALUES.

The optimal control defined by the minimum principle depends on the co-states. The appropriate co-state values are those that produce the correct optimal control from $H_u=0$. The optimal angle-of-attack for the equilibrium is that given either by the energy-layer formulation or that dictated by the optimality condition.

In the energy-layer the angle-of-attack (α) is a control variable but is found from the lift equals weight constraint. In the inner-layer, α is a control to be found from the optimality condition $H_\alpha=0$. Since the energy-layer values must furnish an equilibrium point for the altitude-path angle dy-

namics the two angles-of-attack emerging from these seperate formulations must be equal. In principle, this condition can be used to solve for the missing equilibrium co-state values. However, λ_γ does not appear in the optimality condition, and so it cannot be determined by this approach.

A more elegant approach is to reconsider the energy-layer analysis, now treating the altitude(h) and path angle(γ) as control variables. The conditions

$$V \sin\gamma = 0 \qquad (= \dot{h})$$

$$\frac{g}{V}\left(\frac{L}{W} - \cos\gamma\right) = 0 \qquad (= \dot{\gamma})$$

are treated as equality constraints [4,11] and added on to the Hamiltonian with arbitrary Lagrange parameters λ_h and λ_γ, respectively. The optimality conditions

$$H_h = 0 \quad \text{and} \quad H_\gamma = 0 \,, \quad H = H^0 + H^1 + H^2 \tag{3.1}$$

enable one to determine the values of λ_h and λ_γ. It turns out that $\lambda_h|_{eqm}=0$ and λ_γ has a non-zero value in general. The λ_γ value from this approach is exactly the same as would emerge from the first procedure.

3.3: THE LINEARIZATION PROCESS

The zeroth-order boundary layer equations are :

$$\overset{0}{h} = V \sin\gamma$$

$$\overset{0}{\gamma} = (g/V)\ (L/W - \cos\gamma)$$

$$\overset{0}{\lambda}_h = - \partial H / \partial h$$

$$\overset{0}{\lambda}_\gamma = - \partial H / \partial \gamma$$

where, α and η are determined from

$$H_\alpha = 0 \quad \text{and} \quad H_\eta = 0 \tag{3.2}$$

respectively.

This can be written as (Ref. 4)

$$\overset{0}{x} = g(x,u)$$

$$\overset{0}{\lambda} = - \frac{\partial H}{\partial x}$$

$$H_u\ (x,\lambda,u) = 0 \tag{3.3}$$

where,

$$x = \begin{bmatrix} h \\ \gamma \end{bmatrix}\ ,\ \lambda = \begin{bmatrix} \lambda_h \\ \lambda_\gamma \end{bmatrix} \quad \text{and } u = (\alpha\ \eta)^t$$

The differential equations (3.3) may be linearized to obtain

$$\dot{\delta x} = g_x \, \delta x + g_u \, \delta u$$

$$\dot{\delta \lambda} = - H_{xx} \, \delta x - H_{x\lambda} \, \delta \lambda - H_{xu} \, \delta u \qquad (3.4)$$

It can be noted that

$$\dot{x} = g = H_\lambda \quad \text{so that,} \quad H_{x\lambda} = g_x^t \qquad (3.5)$$

The linearized optimality condition implies that,

$$H_{ux} \, \delta x + H_{u\lambda} \, \delta \lambda + H_{uu} \, \delta u = 0. \qquad (3.6)$$

which may be solved for δu (assuming H_{uu} is non-singular) Combining , one obtains

$$\dot{\delta x} = (g_x - g_u \, H_{uu}^{-1} \, H_{ux}) \, \delta x - g_u \, H_{uu}^{-1} \, g_u^t \, \delta \lambda \qquad (3.7)$$

$$\dot{\delta \lambda} = (-H_{xx} + H_{xu} \, H_{uu}^{-1} \, H_{ux}) \, \delta x - (g_x^t - H_{xu} \, H_{uu}^{-1} \, g_u^t) \, \delta \lambda \qquad (3.8)$$

The coupled linear equations can be written as:

$$\begin{bmatrix} \dot{\delta x} \\ \dot{\delta \lambda} \end{bmatrix} = \begin{bmatrix} A & N \\ K & -A^t \end{bmatrix} \begin{bmatrix} \delta x \\ \delta \lambda \end{bmatrix} \qquad (3.9)$$

Where,

$$A = g_x - g_u \, H_{uu}^{-1} \, H_{ux}$$

$$N = - g_u \, H_{uu}^{-1} \, g_u^t$$

$$K = - H_{xx} + H_{xu} \, H_{uu}^{-1} \, H_{ux}$$

3.4: SUPPRESSION OF INSTABILITIES

As described in [2], the key requirement is that the boundary-layer system have a 'suitably rich' family of stable solutions. Since these ideas can be more thoroughly explained in the linear case (eqn. 3.9) it is worth reiterating the material from [2].

In the case of an initial boundary-layer, the situation is that the specified initial-values of the fast variables (h and γ) do not agree with values that emerge from the outer analysis (h(E) and $\gamma(E)=0$). Since the initial boundary layer is needed to describe the initial transient, it is necessary that the boundary layer solution tend to zero for large times; i.e., exhibit 'stable' behaviour. Because the initial values of h and γ are arbitrary, there must be a two parameter family of such 'stable' solutions.

In the linear case (eqn. 3.9) the (2n X 2n) matrix has the Hamiltonian form. This means that the lower-right block is

the negative-transpose of the upper-left block and that the other two blocks are symmetric matrices.

Hamiltonian matrices exhibit special eigen-structure. As shown in [2], the characteristic polynomial for a system of the type (3.9) will be a $2n^{th.}$ degree polynomial in even powers of λ; i.e., a polynomial in λ^2. It then follows that if λ is an eigenvalue for (3.9), then so is $-\lambda$. The roots are then symmetric about the imaginary axis. Moreover, since the elements of the matrices are real, the roots occur as conjugate pairs, displaying the usual symmetry about the real axis. The symmetry about the imaginary axis has important consequences in the discussion of stabilty.

Specifically, in order to provide for arbitrary initial conditions on the state variables, it is necessary to find n linearly-independent eigenvectors corresponding to the stable eigenvalues (i.e., those with negative real parts). Due to the symmetry, this can be done unless there are eigenvalues with zero real parts. That is, if the system (3.9) has eigenvalues with zero real parts, then it will not be possible to generate n independent eigenvectors.

As shown in [9], an elegant necessary and sufficient condition can be obtained in the case of a scalar system. In that case, the characteristic equation is of the form $\lambda^2 = \text{const.}$ The linearized equations will have non-zero real parts if the strengthened Legendre-Clebsch condition for both the outer and boundary-layer problems are satisfied. In the current

problem there are two boundary-layer state variables and the result of ref.[9] is inapplicable.It was found that this result does not generalize simply : there are cases in the numerical example where the eigenvalues do not have the desired structure even though the Legendre-Clebsch conditon for the outer problem is satisfied. It is not clear why this is so.

Ref [1] gives necessary conditions for a case with two state variables. Even then, the necessary condition is in terms of the coefficients of the characteristic equation. Relating the coefficients to the matrix elements (in terms of H and g and their derivatives) is another matter and no meaningful generalizations are possible. Moreover, these results are applicable only to a two-state system and extension to a general system is not straightforward.

However, a sufficient condition, although not necessary, can be obtained in terms of the system matrices [13].

The system is :

$$\begin{bmatrix} \dot{\delta x} \\ \dot{\delta \lambda} \end{bmatrix} = \begin{bmatrix} A & N \\ K & -A^t \end{bmatrix} \begin{bmatrix} \delta x \\ \delta \lambda \end{bmatrix} = \begin{bmatrix} M \end{bmatrix} \begin{bmatrix} \delta x \\ \delta \lambda \end{bmatrix} \tag{3.10}$$

where, $N^t = N$ and $K^t = K$.

If $[\ y\ z\ ]^t$ represents an eigenvector ($\varepsilon\ C^{2n}$) for (3.10) then,

$$M \begin{bmatrix} y \\ z \end{bmatrix} = \lambda \begin{bmatrix} y \\ z \end{bmatrix} \quad , \quad \text{where } \lambda \text{ is an eigenvalue.} \qquad (3.11)$$

It follows that

$$[\, z^* \mid y^* \,]\, M = -\,\bar{\lambda}\, [\, z^* \mid y^* \,] \qquad (3.12)$$

where, the superscript represents the conjugate-transpose operation.

Combining the two equations,

$$y^* K y + z^* N z = (\lambda + \bar{\lambda})\, y^* z \qquad (3.13)$$

$$\mathrm{Re}(\lambda) \neq 0 \;\rightarrow\; (\bar{\lambda} + \lambda) \neq 0. \qquad (3.14)$$

Since K and N are symmetric, the left-hand sides are real. As $(\lambda+\bar{\lambda})$ is real, so is y^*z is real. If the left-hand side is non-zero, then λ will not have non-zero real parts. Then a sufficient condition for this to be true is :

$$\begin{aligned} &K < 0 \text{ and } N \leq 0 \quad , \text{ or} \\ &K \leq 0 \text{ and } N < 0 \quad , \text{ or} \\ &K > 0 \text{ and } N \geq 0 \quad , \text{ or} \\ &K \geq 0 \text{ and } N > 0 \quad . \end{aligned} \qquad (3.15)$$

For the problem at hand,

$$N = - g_u H_{uu}^{-1} g_u^t \leq 0 \qquad (3.16)$$

So for this problem, the sufficient condition to ensure stability is :

$$K < 0 \quad \text{i.e.,} \quad - H_{xx} + H_{xu} H_{uu}^{-1} H_{ux} < 0.$$

$$\text{or} \quad H_{xx} - H_{xu} H_{uu}^{-1} H_{ux} > 0. \qquad (3.17)$$

It must be noted that this is only a sufficient condition. The necessary condition is not as restrictive as this, but more restrictive than the Legendre-Clebsch condition for the outer problem, which, although necessary, is not sufficient.

CHAPTER 4. RESULTS FOR THE MISSILE EXAMPLE

4.1: INTRODUCTION

In this section results are presented for the linearization procedure applied to a numerical example. Of particular interest is the eigenvalue structure and the several tests discussed earlier.

4.2: THE MODEL

The numerical example used was the ramjet-powered missile of [6]. The details about the aerodynamic model and the propulsion model are explained in the reference cited.

4.3: RESULTS FOR THE OUTER LAYERS.

The cruise and the Energy-layer are investigated in the previous reference. The main results are quoted here for completeness.

CRUISE-DASH

The fuel-flow versus velocity graph shows regions of nonconvexity.This becomes significant when the optimal speed

is examined as a function of $\bar{\lambda}$ (= λ_F/λ_R). With $\bar{\lambda}$ = 0, the optimal speed is the high-speed point. As $\bar{\lambda}$ increases, the importance of fuel-flow increases and the speed decreases to 6250ft/sec at $\bar{\lambda}$ = 8300ft/lb. Then, a small increase in $\bar{\lambda}$ produces a jump in V to about 4100 ft/sec. Again, as $\bar{\lambda}$ increases, the speed goes lower than 4100ft/sec., decreasing to 3770 ft/sec. in the limit as $\bar{\lambda}\to\infty$

In a related problem of minimizing fuel with a specified average speed, one seeks an altitude that minimizes the fuel-flow at the specified speed. If the specified speed happens to be in a nonconvex region of Q(V), then one has to time-share between the two velocities as shown in fig.17 of the reference.

For the model under consideration, there is a region of non-convexity between velocities of approximately 4100 ft/sec. and 6250 ft/sec.

ENERGY-LAYER

The energy analysis specifies the throttle-setting (η) and the altitude-command (h_c) as functions of energy [6]. As in the cruise layer, non-convexity of the hodograph may result in the need to time-share between two operating points (the hodograph co-ordinates are the state-rate $\dot{E}$, and the cost-rate). In the energy layer, this corresponds to "chattering". In a normal case, multiple solutions are possible: the

operating point can be in any of the four quadrants. The operating points of interest lie either in the first quadrant (where energy increases) or the third quadrant (where it decreases). At each energy, the analysis produces an (γ,h_c) pair for both quadrants.

4.4: RESULTS FOR THE INNER LAYER

The altitude-path angle dynamics were investigated in this research. As a first step, the equations were linearized, and the eigen-structure investigated.

Linearization of the boundary-layer equations are fairly straightforward. Most of the partial derivatives can be obtained analytically, although this involves a lot of effort. Special care must be taken to insure that all functional dependences are taken into account while taking the partial derivatives. H_{hh}, however, cannot be easily determined analytically and the derivative has to be obtained numerically.

As explained earlier, due to the Hamiltonian structure of the system matrix, the negative of an eigenvalue is also an eigenvalue, as is its conjugate. So eigenvalues of the form $\pm a$, $\pm ia$ or $\pm a \pm ib$ are possible.

The eigenvalues of the linearized equations were determined for a range of energies from 200 kft. to 700 kft. Roots of the form $\pm ia$ and $\pm a \pm ib$ were found. As discussed earlier, one needs to find a stable solution subspace that is large

enough to possess solutions for any arbitrary initial conditions on the state-variables. If the eigen-structure is of the form ±ia, the region of absolute stablility is just the zero space. In this case the needed 'rich' family of stable solutions cannot be obtained.

Fig.9 shows the locus of the eigenvalues as a function of energy. Since the structure is symmetrical, only the first quadrant is shown. The root-locus does not seem to follow any particular trend. At the lower energies (200 kft. to 250 kft.), the root-structures are ideal with a damping factor of about seven-tenths. At 300 kft., however, the eigenvalues become purely imaginary. Thereafter, there is no definite pattern. This is not entirely unexpected as the model is very intricate and the propulsive and aerodynamic parameteres are complex functions of the altitude and Mach number.

In all the cases examined, the Legendre-Clebsch condition for the energy-layer was satisfied. But, as explained earlier, there were cases where the eigenvalues were purely imaginary, which, ofcourse, shows that the Legendre-Clebsch condition is not sufficient in the general case to guarantee the existence of the 'rich' family of stable solutions. No case was found for which the Legendre-Clebsch for the reduced problem was not satisfied.

The N and K matrices described earlier are, in this problem, of the form:

$$N = \begin{bmatrix} 0 & 0 \\ 0 & -g_\alpha^2 \, H_{\alpha\alpha}^{-1} \end{bmatrix} \qquad (4.1)$$

And,

$$K = \begin{bmatrix} -H_{hh} + H_{h\alpha}^2/H_{\alpha\alpha} + H_{h\eta}^2/H_{\eta\eta} & 0 \\ 0 & -H_{\gamma\gamma} \end{bmatrix} \qquad (4.2)$$

It can be shown that $H_{\alpha\alpha}>0$ and one has $N\leq 0$. So the sufficient condition from eqn.3.17 is that $K < 0$. Since K is diagonal, this means that each diagonal element be negative. The scalar quantity ($-H_{\gamma\gamma}$) was found to be negative in all the cases examined. The sufficient condition is, then, that the (1,1) element of the matrix K hereafter referred to as K_{11}, be negative. In the numerical test, this condition was not always met.

Our analysis permits us to concude that if K_{11} is negative, then the stability roots will have the proper structure. If, on the other hand, K is not negative-definite, then nothing can be concluded as the negative-definiteness of K is sufficient but not necessary for obtaining the proper structure. In fact, the numerical tests revealed no case where K_{11} was positive with the proper root structure. It should be noted that the magnitude of K_{11} was usually of the order of 10^{-10}

K_{11} is the second order necessary condition for the minimization of the Hamiltonian with respect to altitude, with

the equality constraint that $H_\alpha = 0$. That is, this quantity is :

$$- H_{hh} \,|_{H_\alpha = o}$$

To establish this fact, one notes that for these purposes the Hamiltonian is a function of the states h and γ and the controls α and η. The energy E and all the co-states are fixed for this discussion. Observe that whereas h and γ are independent variables, the controls are dependent upon h (or γ) through the optimality conditions ($H_\alpha=0$ and $H_\eta=0$). Since η and α depend implicitly on h, one calculates the 'constrained' derivative via the chain rule. It is convenient to express this in the 'operator' form as :

$$\frac{\partial(\ )}{\partial h}\Big|_C = \frac{\partial(\ )}{\partial h} + \frac{\partial \alpha}{\partial h}\frac{\partial(\ )}{\partial \alpha} + \frac{\partial \eta}{\partial h}\frac{\partial(\ )}{\partial \eta}$$

The 'coefficients' $\partial\eta/\partial h$ and $\partial\alpha/\partial h$ are found from the (vector) constraint, $H_u=0$. In general, this results in

$$\frac{\partial u}{\partial h} = -\left[H_{uu} \right]^{-1} \frac{\partial H_u}{\partial h}$$

or in component form

$$\begin{bmatrix} \frac{\partial \eta}{\partial h} \\ \frac{\partial \alpha}{\partial h} \end{bmatrix} = \begin{bmatrix} H_{\eta\eta} & H_{\eta\alpha} \\ H_{h\alpha} & H_{\alpha\alpha} \end{bmatrix}^{-1} \begin{bmatrix} H_{\eta h} \\ H_{\alpha h} \end{bmatrix} \qquad (4.4)$$

For the current problem, the cross-derivative $H_{\eta h}$ is zero so that the result simplifies to :

$$\partial \eta / \partial h = - H_{\eta h} / H_{\eta \eta}$$

and

$$\partial \alpha / \partial h = - H_{\alpha h} / H_{\alpha \alpha} \qquad (4.5)$$

Using the chain rule twice, one obtains the second derivative as:

$$- H_{hh}|_C = - H_{hh} + H_{h\alpha}/H^2_{\alpha\alpha} + H_{h\eta}/H^2_{\eta\eta} \quad . \qquad (4.6)$$

The Legendre-Clebsch condition for the reduced problem is :

$$- H_{hh} \mid_{L=W} < 0 \qquad (4.7)$$

This is different from the sufficient condition in that the equality constraint is different. Expanding (4.6), one finds

$$H_{hh} \mid_{L=W} = H_{hh} + 2 H_{h\alpha} L_h / L_\alpha - H_{\alpha\alpha} L^2_h / L^2_\alpha \quad . \qquad (4.8)$$

In the sufficient condition, the terms are of the same order and of the same sign, and so the difference could be

positive or negative. This is what causes the non definiteness of the matrix K.

Two cases are examined in more detail. At 200 Kft. of energy, the eigenvalues have the desired structure. At 300 Kft., the eigenvalues are all purely imaginary. At these energies the second derivative of the Hamiltonian is explored in more detail. The derivatives were found analytically and verified numerically (except the explicit second derivatives with respect to h, which were found only numerically). The following are the relevant values:

At 200 kft.

$$H_{hh} \mid_{\text{unconstained}} = \quad 0.263\ E{-}07$$

$$H_{h\alpha}^2/H_{\alpha\alpha} + H_{h\eta}^2/H_{\eta\eta} = \quad 0.617\ E{-}10$$

$$2\, H_{h\alpha}\, L_h / L_\alpha - H_{\alpha\alpha}\, (L_h/ L_\alpha)^2 = \quad 0.427\ E{-}10$$

$$H_{hh} \mid_{L=W} = \quad 0.267\ E{-}07$$

$$H_{hh} \mid_{H_\alpha=0} = \quad 0.262\ E{-}07$$

At 300 Kft.,

$$H_{hh} \mid_{\text{unconstained}} = -\ 0.162\ E{-}09$$

$$H_{h\alpha}^2/H_{\alpha\alpha} + H_{h\eta}^2/H_{\eta\eta} = 0.289\ E-09$$

$$2\ H_{h\alpha}\ L_h\ /\ L_\alpha - H_{\alpha\alpha}\ (L_h/\ L_\alpha)^2 = 0.362\ E-10$$

$$H_{hh}\ |_{L=W} = 0.200\ E-09$$

$$H_{hh}\ |_{H_\alpha=0} = -\ 0.191\ E-09$$

It is seen that at 300 Kft., the unconstrained derivative is negative but the add-on part due to the constraint L=W makes it positive. On the other hand, the add-on part in the inner-layer is of the wrong sign and makes the total derivative still more negative. The K_{11} element in this case is thus positive. At 200 Kft., the unconstrained derivative is positive and large enough to counter the effects of the constraints.

4.5: ARDEMA'S NECESSARY CONDITION

As described in Ardema [1], for a Hamiltonian system with two state variables, the characteristic equation is of the form :

$$\lambda^4 + K_2\ \lambda^2 + K_1 = 0. \qquad (4.9)$$

The proper eigen-structure is obtained when

$$4 K_1 > K_2^2$$

$$K_1 > 0 \quad \text{and} \quad K_2 > 0 .$$

For the problem at hand, the first condition is the relevant one. In terms of the derivatives of the Hamiltonian, this condition translates to :

$$a + b + c + d > 0 , \tag{4.10}$$

where,

$$a = 4 (g^1_\gamma)^2 (g^2_\alpha)^2 H_{hh} / H_{\alpha\alpha}$$

$$b = - 4 g^1_\gamma g^2_\alpha (H_{h\alpha}^2 / H_{\alpha\alpha}^2 + H_{h\eta}^2 / H_{\eta\eta}^2)$$

$$c = 4 g^1_\gamma g^2_h (g^2_\alpha)^4 / H_{\alpha\alpha}^2$$

$$d = - 4 g^1_\gamma (g^2_\alpha)^5 H_{h\alpha} / H_{\alpha\alpha}^3$$

$$e = (g^2_\alpha)^4 H_{\gamma\gamma}^2 / H_{\alpha\alpha}^2$$

where,

$$g^1 = \dot{h} = V \sin\gamma$$

$$g^2 = \dot{\gamma} = (g/V)\ (L/W - \cos\gamma)$$

The lack of an appropriate eigen-structure means that the problem does not exhibit the time-scale structure assumed in the singular-perturbation formulation. Boundary-layer-like transients do not exist in such cases; in fact there are fast oscillations that do not die out. One way to circumvent this difficulty is to alter the problem by introducing an additional 'artificial' cost term of the form $K\ \delta h^2$, with K (a positive constant) to be determined. Clearly this additional term changes the unconstrained second derivative of the Hamiltonian by an additive factor of K. By proper choice of this 'weight', one can guarantee the proper structure for the linearized boundary-layer stability roots.

CHAPTER 5. FEEDBACK ANALYSIS

5.1: INTRODUCTION

In this chapter, selection of the initial conditions on the multipliers to suppress the unstable modes is discussed, and, feedback laws from the linearized model are generated. Sample altitude path-angle trajectories are obtained with the feedback laws. For comparison, the NL2PBVP of section 2.5 is solved. Finally the integration of the feedback laws for the angle of attack into a full trajectory generator is discussed.

5.2: SELECTION OF MULTIPLIERS

The initial value of the multipliers λ_h and λ_γ are free parameters. In the h-γ zeroth order boundary layer (cf. eqn.2.10) these are selected to produce the asymptotic fairing from (arbitrary) given initial values of the states h and γ to the energy layer values ($h=h_c(E)$ and $\gamma=0$). In the linearized model the choice of initial λ_h and λ_γ is more straightforward : they are selected to suppress unstable modes. A general procedure for doing this is now presented. It should be noted that the approach is closely related to

Potter's method [10] for finding the steady-state solution of a linear-quadratic regulator problem.

From eqn.(3.9) the coupled state-adjoint linear system is:

$$\begin{bmatrix} \dot{x} \\ \dot{\lambda} \end{bmatrix} = \begin{bmatrix} A & N \\ K & -A^t \end{bmatrix} \begin{bmatrix} x \\ \lambda \end{bmatrix} \tag{5.1}$$

It should be noted that x and λ are perturbation quantities. The δ prefix has been temporarily dropped.

It is assumed that the 2nx2n Hamiltonian matrix on the right-hand side of (5.10) ha n eigenvalues with positive real parts and n with negative real parts (and none with zero real parts). The eigenvalues are collected in a modal matrix by arranging those eigenvectors corresponding to eigenvalues with positive real parts in the first n columns and those corresponding to eigenvalues with negative real parts in the last n columns. One then writes the modal matrix in partitioned form as:

$$W = \begin{bmatrix} W_{11} & W_{12} \\ W_{21} & W_{22} \end{bmatrix} \tag{5.2}$$

where each block is an nxn matrix. In modal co-ordinates, the linear system (5.1) is written as:

$$\begin{bmatrix} \dot{Z}_1(t) \\ \dot{Z}_2(t) \end{bmatrix} = \begin{bmatrix} \Lambda & 0 \\ 0 & -\Lambda \end{bmatrix} \begin{bmatrix} Z_1 \\ Z_2 \end{bmatrix} \tag{5.3}$$

where Λ is a diagonal matrix of eigenvalues with positive real parts. Since the system (5.3) is decoupled, it is easily seen that the Z_1 component will exhibit exponential growth (as $t\to\infty$) while the Z_2 component will exponentially decay. To suppress the Z_1 part, one must have the initial condition $Z_1=0$. This can be written in terms of the original (x,λ) co-ordinates using the modal transformation matrix (5.2). Specifically one has

$$\begin{bmatrix} x \\ \lambda \end{bmatrix} = W \begin{bmatrix} Z_1 \\ Z_2 \end{bmatrix}$$

or

$$\begin{bmatrix} Z_1 \\ Z_2 \end{bmatrix} = W^{-1} \begin{bmatrix} x \\ \lambda \end{bmatrix}$$

Writing V for W^{-1} and partitioning as before, the condition for suppressing the instabilities is:

$$V_{11}\, x(t_o) + V_{12}\, \lambda(t_o) = 0 \tag{5.4}$$

or formally,

$$\lambda(t_o) = - V_{12}^{-1}\, V_{11}\, x(t_o) \tag{5.5}$$

Equation (5.5)is one form of the working equation that can be used to determine the initial values for the co-states in terms of the states. In general, one must prove that the V_{12} matrix in (5.4) has an inverse so that equation (5.5) makes

sense. This is done in [10] (pages 243-248). In fact it is shown in [10] that (5.5) is equivalent to :

$$\lambda(t_o) = - W_{22} W_{12}^{-1} x(t_o) \qquad (5.6)$$

so that one need not invert the complete modal matrix. While eqn.(5.6) involves complex matrices (generally), one can avoid this by using the conjugate structure since the Hamiltonian has only real entries (see, for example pp.250-251 in [10]).

Figs 5-8 show the multipliers estimated by the above procedure compared with the exact multipliers obtained by solving the NL2PBVP. The estimates seem to agree very well with the exact solutions. This is in contrast with Ardema's results [1] where the region of agreement was negligibly small. The estimates agree even with a large perturbation such as 8000 ft. altitude perturbation or a 0.4 rad. path-angle disturbance.The equilibrium values are 13,100 ft. and 0 rad., respectively. In spite of the initial misgivings about the usefulness linearization, these excellent results engendered a renewed interest in the possibility of a linearized feedback scheme, particularly in view of on-board application.

5.3: FEEDBACK LAWS

The analysis of the previous section provides the co-state perturbations required to suppress (linear) instability for a given state perturbation. As noted in chapter 3, the linearized optimality condition is:

$$H_{ux}\,\delta x + H_{u\lambda}\,\delta\lambda + H_{uu}\,\delta u = 0 \qquad (5.7)$$

This can be solved (assuming non-singular H_{uu}) to yield

$$\delta u = -H_{uu}^{-1}\,(\,H_{ux}\,\delta x + H_{u\lambda}\,\delta\lambda\,) \qquad (5.8)$$

Now, using the derived condition (5.6), one finds

$$\delta u = -H_{uu}^{-1}\,\left[\,H_{ux} + H_{u\lambda}\,W_{11}\,W_{12}^{-1}\,\right]\,\delta x\ . \qquad (5.9)$$

This is a (linearized) feedback law for control perturbations in terms of state perturbations. For the problem at hand, the control vector u has two components (α and η) and the H_{uu} matrix is diagonal. In addition, since the throttle setting does not appear in the system equations (3.2) the second row of $H_{u\lambda}$ is identically zero.

For the angle-of-attack control,

$$B\,\delta\alpha(t) = -N\,\lambda(t). \qquad (5.10)$$

For the linearized system, the B matrix is :

$$B = \begin{bmatrix} 0 \\ \\ (g/VW)L_{\alpha} \end{bmatrix} \tag{5.11}$$

and so,

$$B\ \delta\alpha = \begin{bmatrix} 0 \\ \\ (g/VW)L_{\alpha} \end{bmatrix} \delta\alpha = -\ N\ (\ W_{22}\ W_{12}^{-1}\ )\ x(t). \tag{5.12}$$

Calling the second element of B as B_2, then,

$$\delta\alpha = -\ (\ 1\ /\ B_2)\ \{ \begin{bmatrix} N\ W_{22} & W_{12}^{-1} \end{bmatrix} \begin{bmatrix} \delta h \\ \delta\gamma \end{bmatrix} \}_2 \tag{5.13}$$

where the subscript on the matrix indicates the second element.

$$\text{i.e., } \delta\alpha = f_1\ \delta h + f_2\ \delta\gamma \ \rightarrow\ \alpha = \alpha_o + f_1\ \delta h + f_2\ \delta\gamma. \tag{5.14}$$

This is then, the required feedback control for the angle-of-attack that generates an approximate trajectory.

For the throttle-setting, as mentioned earlier, $H_{\eta\lambda}$ is identically zero. The resulting throttle-setting was found to be accurate in a very small region. But it was found for one case (200 kft.), the optimal throttle varied by less than 1.5% over a 8000 ft. perturbation. So one solution is to regard the throttle constant (at the equilibrium value) .

5.4: ALTITUDE / PATH-ANGLE TRANSIENTS

One way to demonstrate the usefulness of the linearized analysis is to compare the solutions it produces with that of the 'exact' boundary value problem. It should be noted that this dicussion pertains to the zeroth-order h-γ boundary layer approximations (2.10) (i.e., energy is constant). The 'exact' solution was generated using a multiple-shooting algorithm [5]. The particular package used integrates the equations with a Runge-Kutta-Fehlberg (7-8 th. order) method. It uses a modified Newton's method to update the values of the dependent variables at specified grid-points. This method needs a good estimate of the solution and, as it was not known a priori how good the linearized solution would be, it was not used as a first approximation. Starting with the equilibrium values of the states (from energy layer) and the costates (obtained as in section 3.2), the equations were solved backward in time for a sample trajectory. This does not always work as the state equations are unstable and the trajectory may not get where one wants it to go. It has to be done with patience and care. Then, with a fairly good estimate, one can solve the equations with the split boundary conditions.

As stated earlier, all the four equations were integrated and H = constant was used as a check. But, during the solution the equations using the feedback control, only the state

equations were integrated, since they are independent of the co-states, (Only the control depends on the co-states, which are indirectly estimated). It is noted that the equations are still nonlinear. Only the feedback law is linear. So the equations must be numerically integrated with a good method (like Verner's 4-5th. order Runge-Kutta method).

For simulation, an energy of 200 Kft. with the equilibrium conditions h≈13,100 ft. and, of course, γ=0 was considered Sample trajectories are presented in Figs 1-4. Figs 1 and 2 correspond to the initial conditions of δh=8000 ft. , $\delta\gamma$=0.1 and figs. 3 and 4 correspond to the initial conditions δh=4000 ft. , $\delta\gamma$=0.4. The exact histories of altitude and path-angle are shown in comparison with the feedback solution. The agreement seems to be remarkably good.

The advantages of using the linear feedback control are obvious. One does not need to solve a two-point boundary value problem. Moreover, one does not have to integrate the co-states, whose derivatives are the more involved ones. The feedback facilitates an on-board application, which would be impossible with the exact method.

5.5: COMPLETE TRAJECTORY ANALYSIS

The complete trajectory with the zeroth-order approximation is the composite solution obtained in the manner of [9]. This (the Vasil'eva composite as referred to in [9])

is the combination of the solutions for the cruise, energy and the inner layers.

As described in [6], the energy transition analysis provides two solutions for the controls ($h_c(E)$, $\eta_c(E)$, $\alpha_c(E)$, $\gamma=0$) at each energy. One of these produces an energy gain (first quadrant in the corresponding hodograph), while the other produces energy-loss (third quadrant).

The linearized altitude / path-angle analysis has resulted in first-order corrections to the angle-of-attack :

$$\alpha(E,h,\gamma) = \alpha_c(E) + K_{\alpha h}(E)\ (h-h_c(E)) + K_{\alpha\gamma}(E)\ \gamma \qquad (5.15)$$

The functions of energy may be separated by 'solving' the linearized problem of chapter 4 at a collection of energies and then employing some form of table look-up and interpolation. Before proceeding further along this line, there are some remarks that need to be made about integrating the feedback scheme into a trajectory generator.

Firstly, the feedback scheme has been obtained for a particular vehicle weight, while in on-board applications, the weight of the vehicle changes with time. One way to compensate feedback scheme for weight variation is to determine the load-factor with the feedback, rather than the angle-of-attack. Then, the angle-of-attack can be determined appropriate for the current weight. For this, as before:

$$n(E,h,\gamma) = 1 + K_{nh}(E)\ (h-h_c(E)) + K_{n\gamma}(E)\ \gamma \qquad (5.16)$$

In this problem, the perturbation terms for the throttle setting were neglected i.e., the throttle was taken as the energy layer throttle command.

A second problem is that there are gaps in the look-up table where the linearized equations are not stable. The these must be filled, theoretically, with "averaging" analysis, not yet developed.

As a first step one can turn a blind eye and interpolate for the gains at energies where the data is not available. It must, however, be stressed that there is no theoretical justification for this. An alternative procedure is to augment the cost with the penalty $k\delta h^2$. This then, will affect the H_{hh} term and will produce desirable roots for the system. Fig.(11) shows the effect of the penalty parameter (K) on the roots at 300 Kft. of energy. Apparently one can select gains that provide roots with desirable damping characteristic.

This procedure was carried out for the missile example. As discussed earlier, there are two cruise points. Different average velocities are obtained by time-sharing between the two cruise points. Several trajectories were run with the model of Ref.[6].

It was found that for large energy transients, such as in climb, the linear-feedback control produced large oscillations that sometimes caused the missile to hit the ground.

Since the altitude / path-angle analysis is based on a linear model, and because of the aforementioned gaps, failure of the controller for large disturbances is not unexpected. Such instability during the climb-out was encountered during the study reported in [6] when a linear feed-back was used. In that work, [6], the difficulty was overcome by employing an ad-hoc load-factor feedback law for large disturbances (in $h-h_c$ and γ) and switching to a linearized version only when the disturbances had decreased. The same procedure was adopted for the current simulation. The important new feature is that the linearized law is now based on the optimization procedure.

For all the simulations, the initial conditions were 2830 ft. , 0.436 rad. and 200 kft. for altitude, path angle and energy, respectively. The different average velocities were obtained by varying the amount of time the missile 'resided' in the higher-velocity cruise point. For the same residence time, trajectories were run with the ad-hoc procedure of Ref.(6), the interpolated gains and the gains manipulated by the penalty parameter to give about seven-tenths damping ratio.

Fig.12 shows the plot of range obtained against the average speed. The range obtained with the manipulated gains appears to compare well with the ad hoc procedure.

Fig.13 is a plot of the trajectories for an illustrative case. The plot shows the altitude history as function of the

range for the case where the cruise point 'resided' at the higher energy point for 50 sec. The trajectories with the ad-hoc procedure, the interpolated gains and the manupulated gains are shown superimposed for comparison. For the case with interpolated gains, the missile ran out of fuel when the simulation stopped, but it was headed for certain disaster.

CHAPTER 6. CONCLUSION

6.1: DISCUSSION OF RESULTS

The cruise-dash optimization problem for an aircraft has been studied with singular-perturbation analysis. The problem has been broken down to three separate sub-problems. The inner boundary-layer has been analyzed in detail.

Linearization has been applied to solve the altitude-path angle dynamics. It has been shown that the linearized equations are not always stable. It has been shown that Kelley's sufficient condition for the scalar-state-variable case [9] is no longer sufficient when there are two or more states. A sufficient condition involving the positive and/or negative definiteness of the partitioned matrices has been obtained. Comparison with Ardema's necessary has been provided.

The generation of the feedback scheme has been detailed. For the numerical example of a missile, the feedback laws have been generated. It has been shown that the altitude / path-angle transients with these feedback laws approximates the 'exact' trajectory very well.

6.2: SUGGESTIONS FOR FURTHER STUDY.

This study had basic restrictive assumptions, one of the most important of which is that weight of the airplane is assumed to be constant. This, however, affects only the outer layer. Still it seems worth-while to study the effects of a weight-varying airplane. The assumption of thrust-along-the-path is another assumption which only simplifies the algebra and is not very restrictive.

The solutions obtained were all zeroth order solutions for the boundary layer equations. The obvious next step is to consider higher order solutions to better account for transitions.

As shown, difficulties arise when the instabilities in the linearized boundary-layer cannot be suppressed. Such cases may be prime examples for averaging and periodic-optimal-control methods.

LIST OF REFERENCES.

1. Ardema, M.D.,"Linearization of the Boundary-Layer Equations of the Minimum Time-to-Climb Problem" J. Guidance and Control, (2) 1979, pp.434-436

2. Ardema, M.D.,Singular Perturbations in Flight Mechanics ,NASA TM X-62380, July 1977 (Revised Edition).

3. Bilimoria, K.D., Cliff, E.M. and Kelley, H.J., "Classical and Neo-Classical Cruise-Dash Optimization", Journal of Aircraft, July 1985.

4. Bryson, A.E. and Ho, Y.C.,Applied Optimal Control, Hemispere,1975.

5. Bulirsch, R.,"Einfuhrung in die Flugbahnoptimatierung die Mehrzielmethode zur Numerischen Losung von Nichtlinearen Randwertproblemen und Aufgaben der Optimalen Steuerung.", Lehrgang Flugbahnoptimierung Carl-Cranz-Gesellschaft e.v.,October 1971.

6. Cliff, E.M., Kelley, H.J. and Lutze, F.H.,A Sudy of Systems optimization Applied to Surface-Air Missile Operations,V.P.I.&S.U. Report to NSWC, March 1985.

7. Collins, B.P., Haines, A.L. and Wales, C.J.,"A Concept for a Fuel Efficient Flight Planning Aid for General Aviation", NASA CR 3533.

8. Houlihan, S.C., Cliff, E.M., and Kelley, H.J.,"A Study of Chattering Cruise", in Journal of Aircraft, Vol.13, october 1976, pp 828-830.

9. Kelley, H.J.,"Aircraft Maneuver Optimization by Reduced Order Approximation",Control and Dynamic Systems,Vol. 10, C.T.Leondes, ed., Academic Press, 1973.

10. Kwakernaak, H. and Sivan, R.,Linear Optimal Control Systems,Wiley-Interscience,1972

11. Leitmann, G.,An Introduction to Optimal Control, McGraw- Hill, 1966.

12. Knox, C.E.,"Application of Fuel/Time Minimization Techniques to Route Planning and Trajectory Optimiza-

tion", NASA Aircraft Controls Research,NASA Conference Publication 2296 , Beasley, G.P., ed., October 1983.

13. Paige, C. and Van Loan, C.,"A Schur Decomposition for Hamiltonian Matrices ",Linear Algebra and its Applications, Vol.41, 1981.

14. Weston, A.R., Cliff, E.M. and Kelley, H.J.,"On-Board Near-Optimal Climb-Dash Energy Management" in J. of Guidance and Control , Vol.8, May-June 1985.

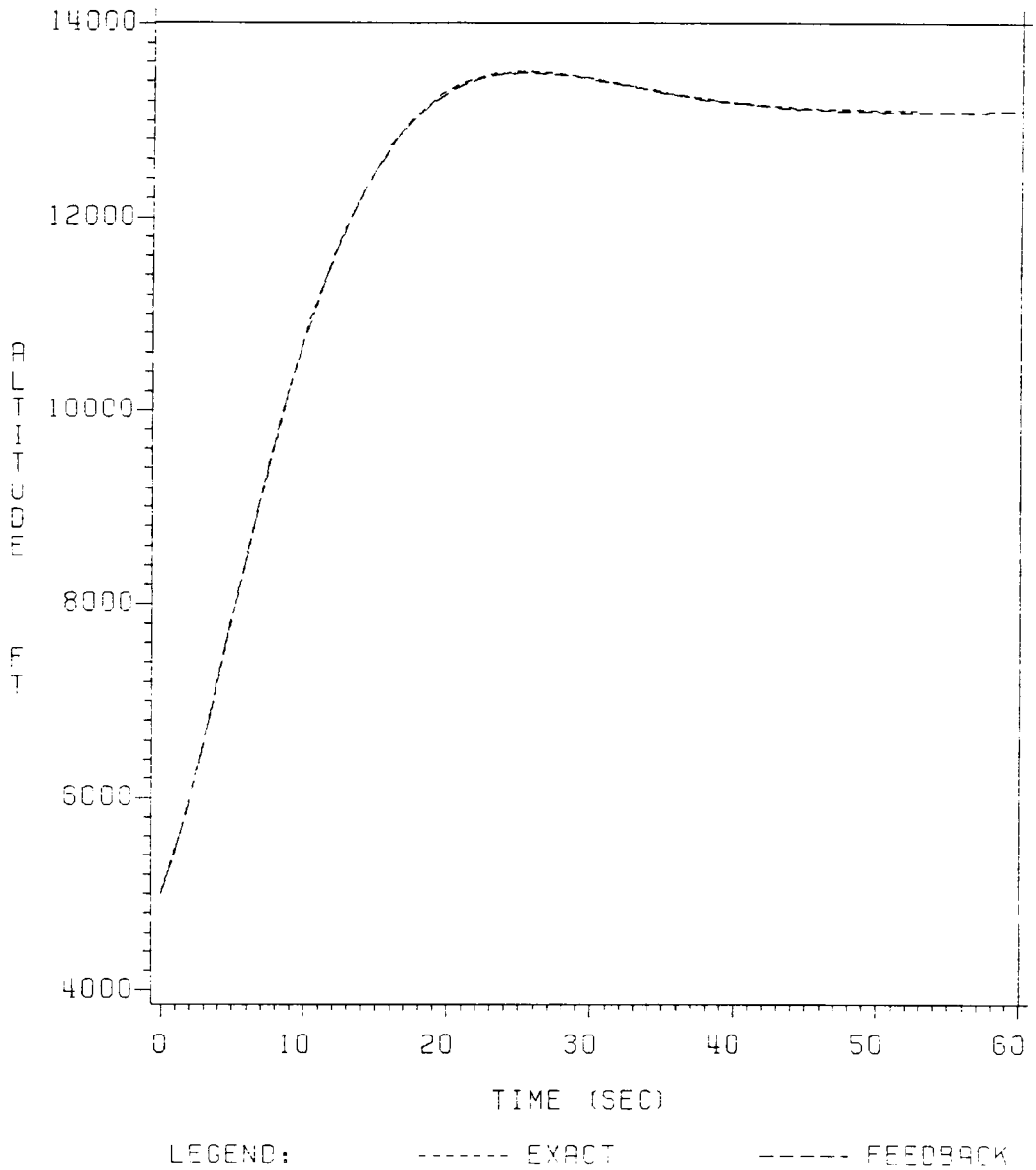

Figure 1. Comparison of Altitude Histories (case A)
h_o=5 kft., γ_o=0.1 rad, E=200 kft.

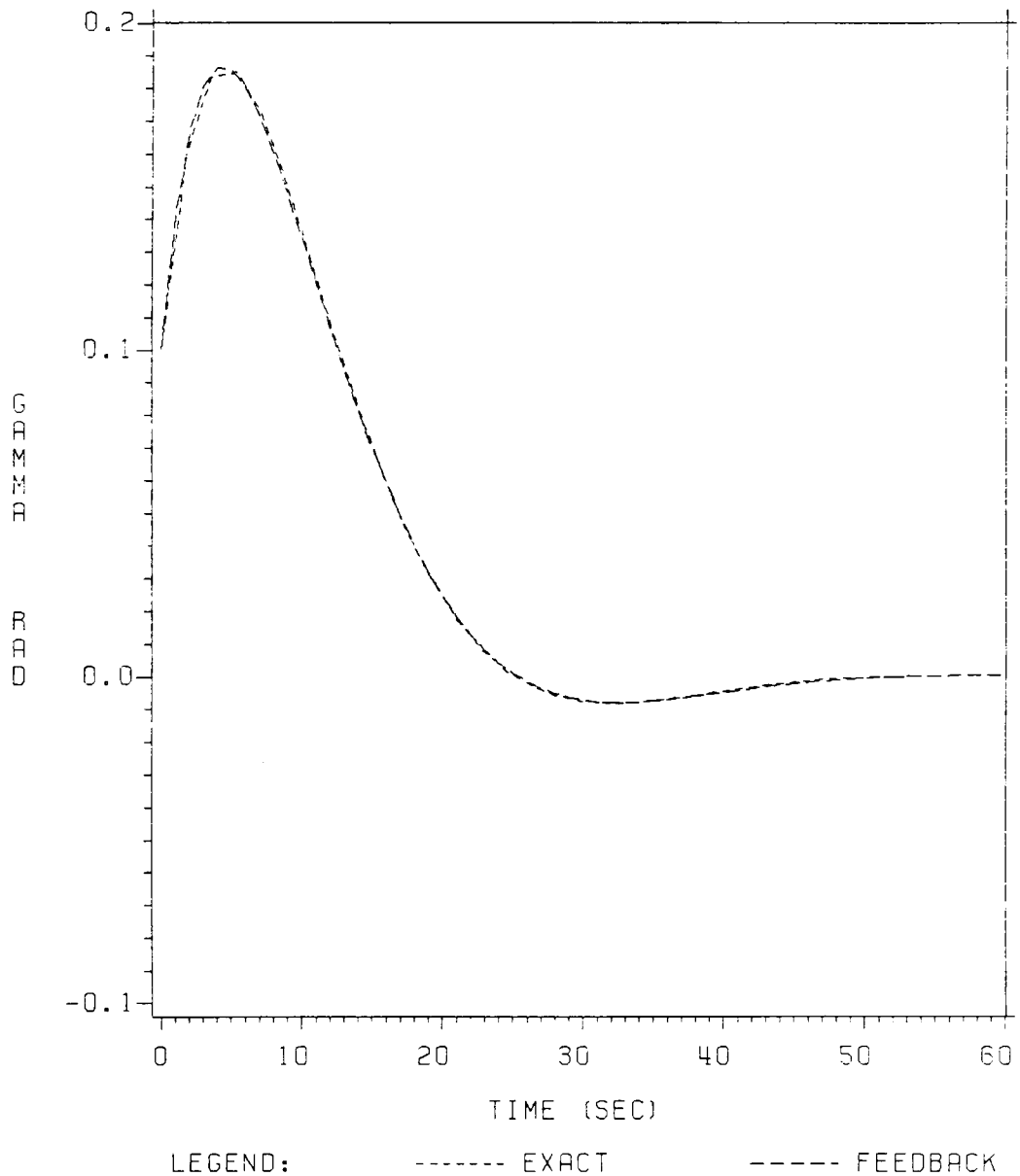

Figure 2. Comparison of Path-Angle Histories (case A)
h_o=5 kft., γ_o=0.1 rad, E=200 kft.

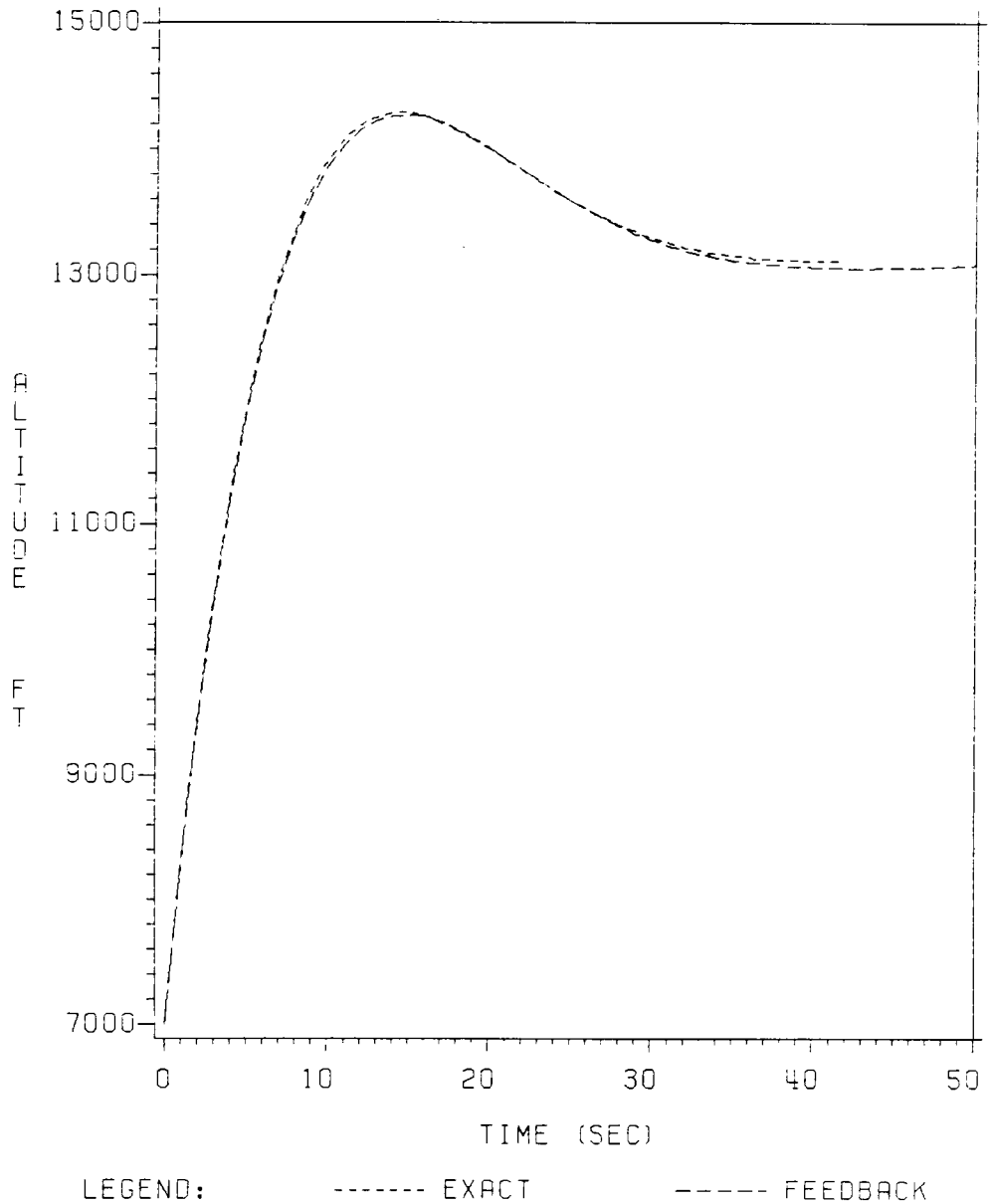

Figure 3. Comparison of Altitude Histories (case B) h_o=7 kft., γ_o=0.4 rad, E=200 kft.

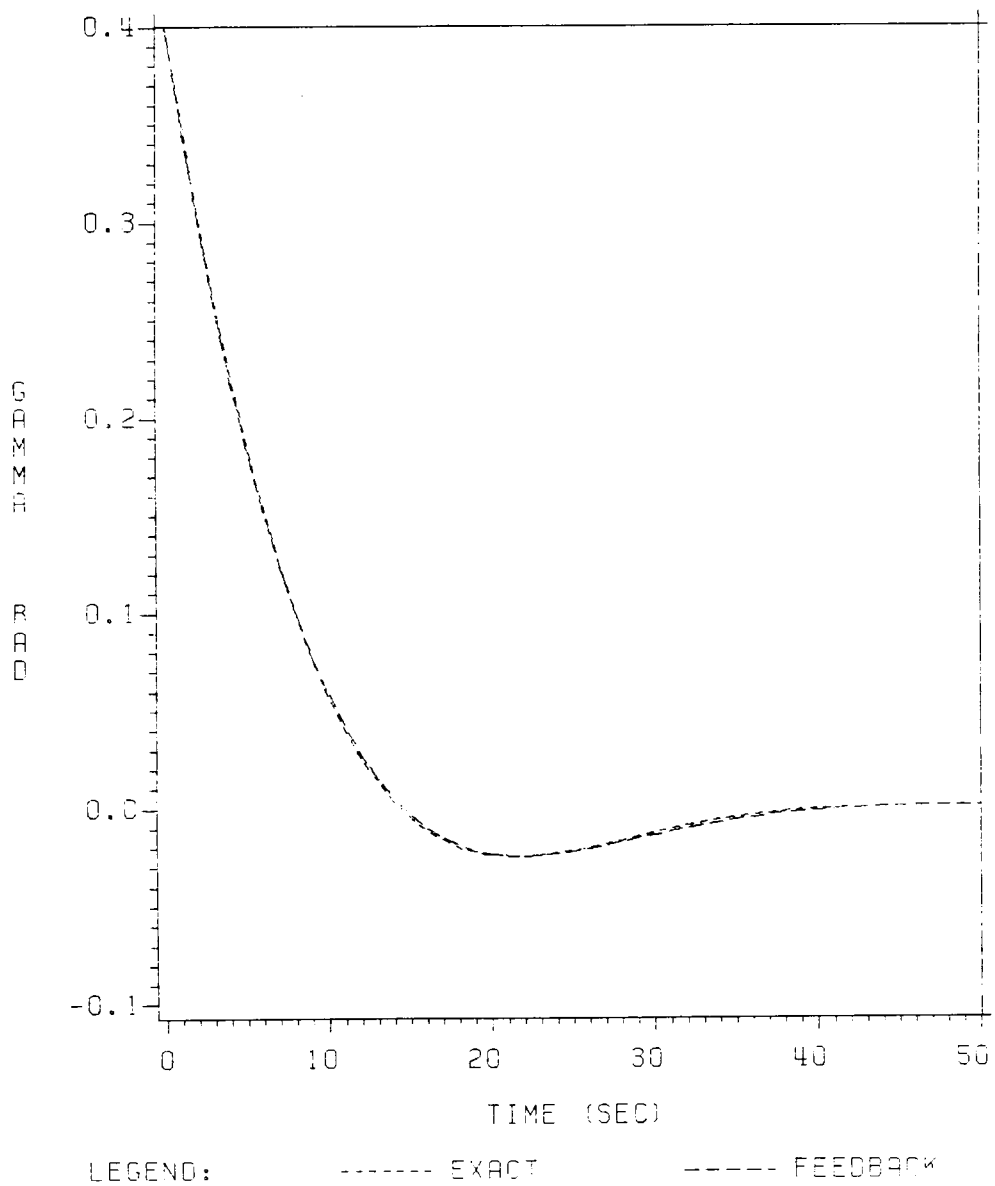

Figure 4. Comparison of Path-Angle Histories (case B) h_o=7 kft., γ_o=0.4 rad, E=200 kft.

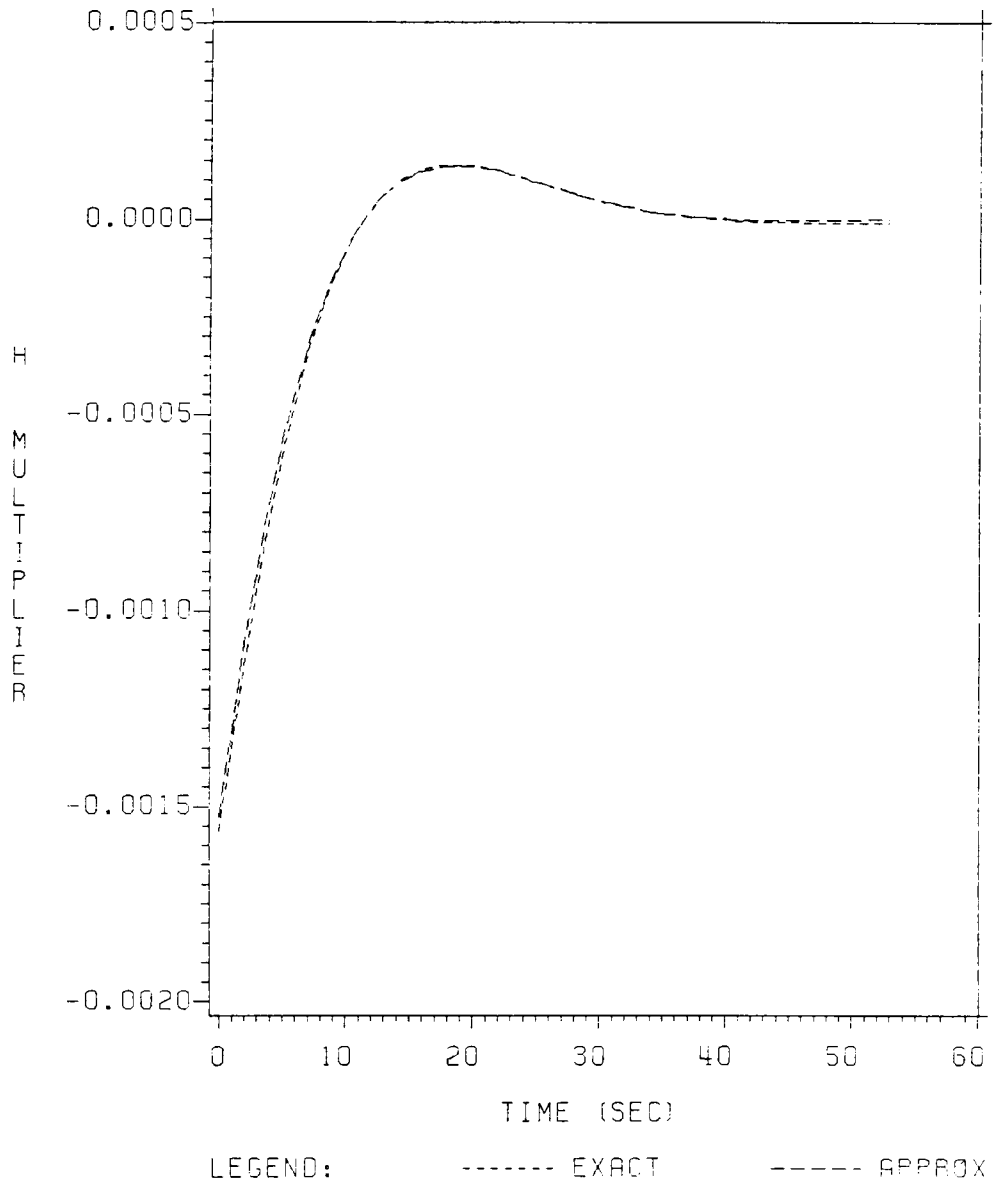

Figure 5. Comparison of h-Multipliers (case A)
h_o=5 kft., γ_o=0.1 rad, E=200 kft.

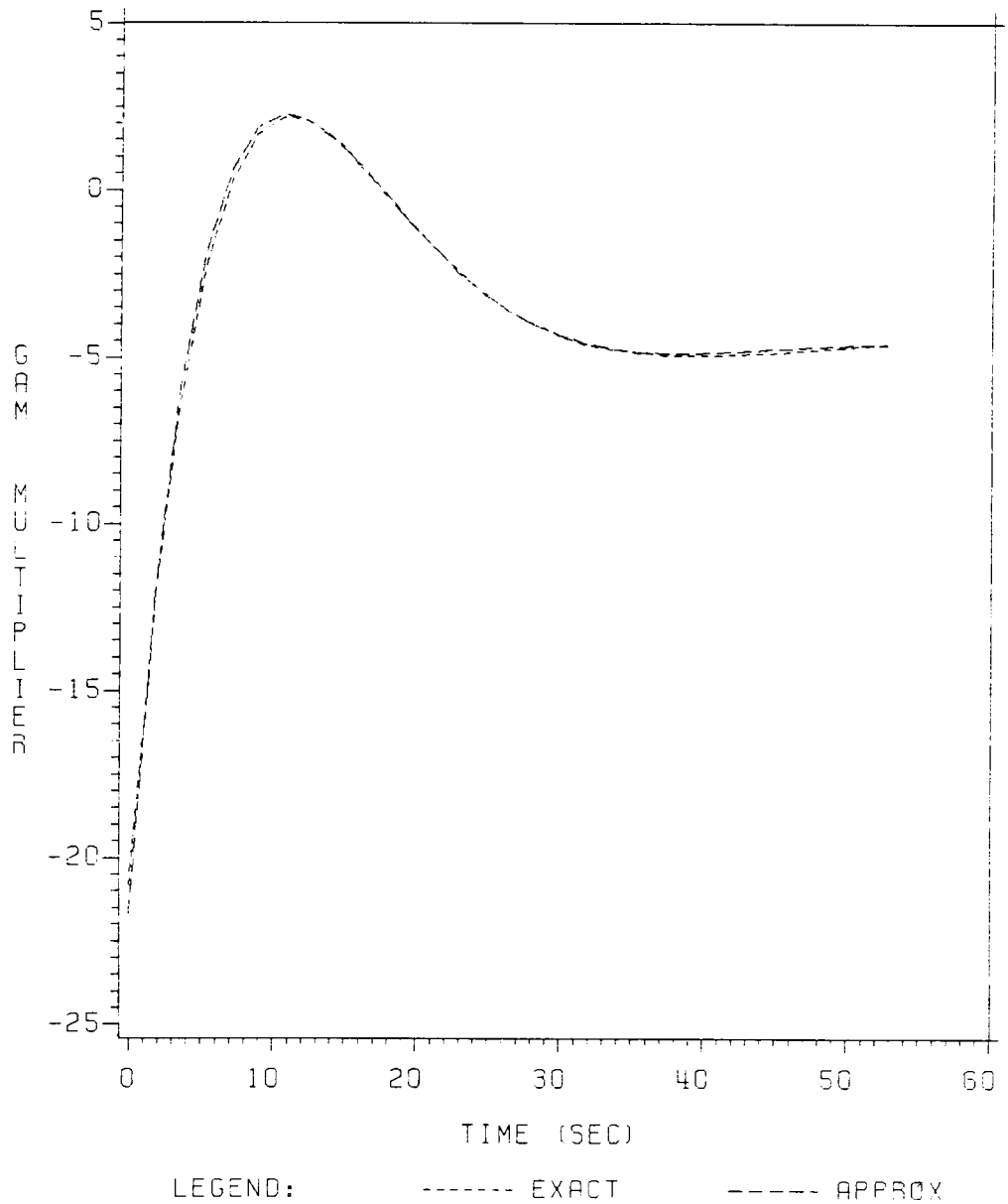

Figure 6. Comparison of γ-Multipliers (case A)
h_o=5 kft., γ_o=0.1 rad, E=200 kft.

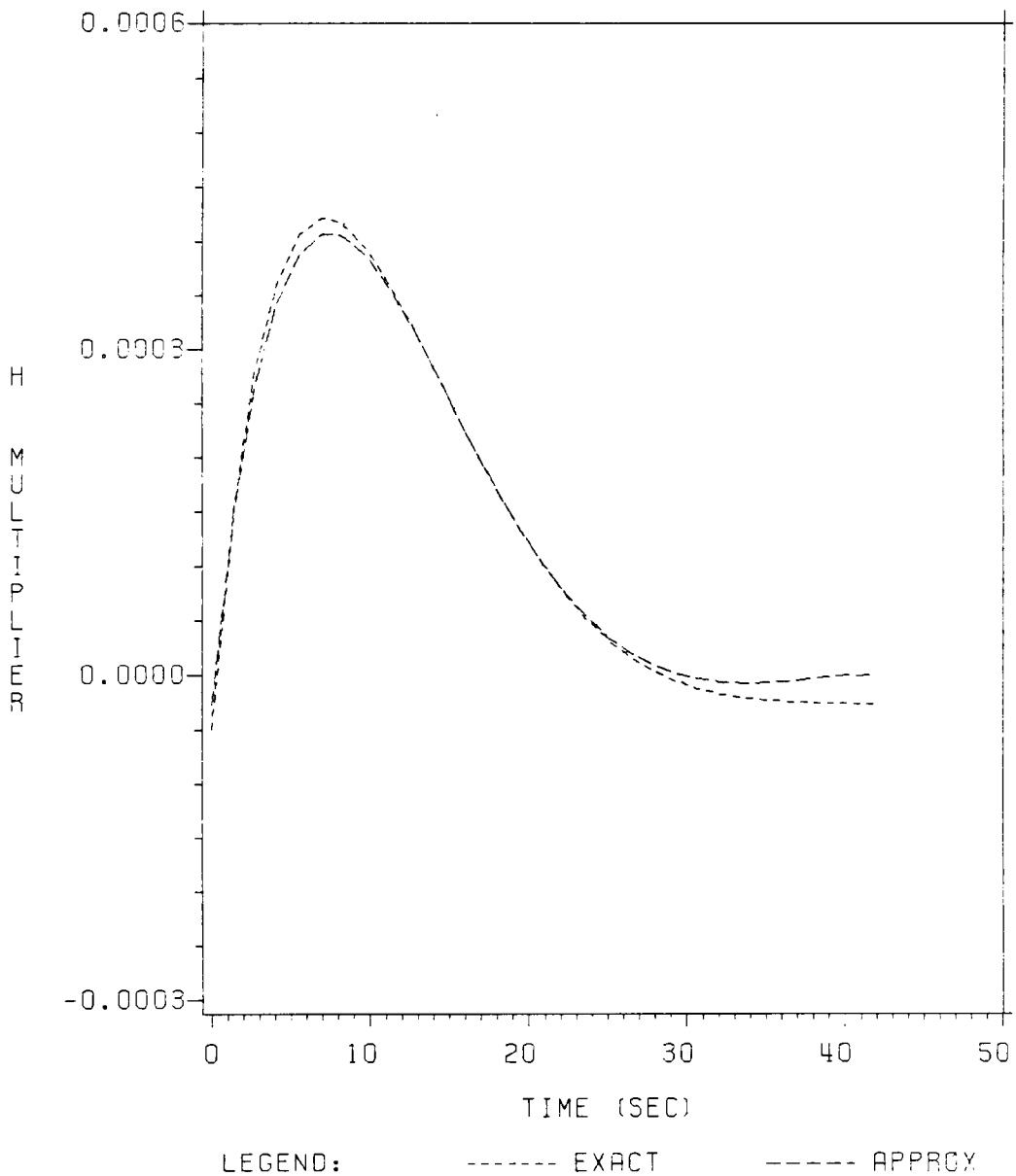

Figure 7. Comparison of h-Multipliers (case B)
h_o=7 kft., γ_o=0.4 rad, E=200 kft.

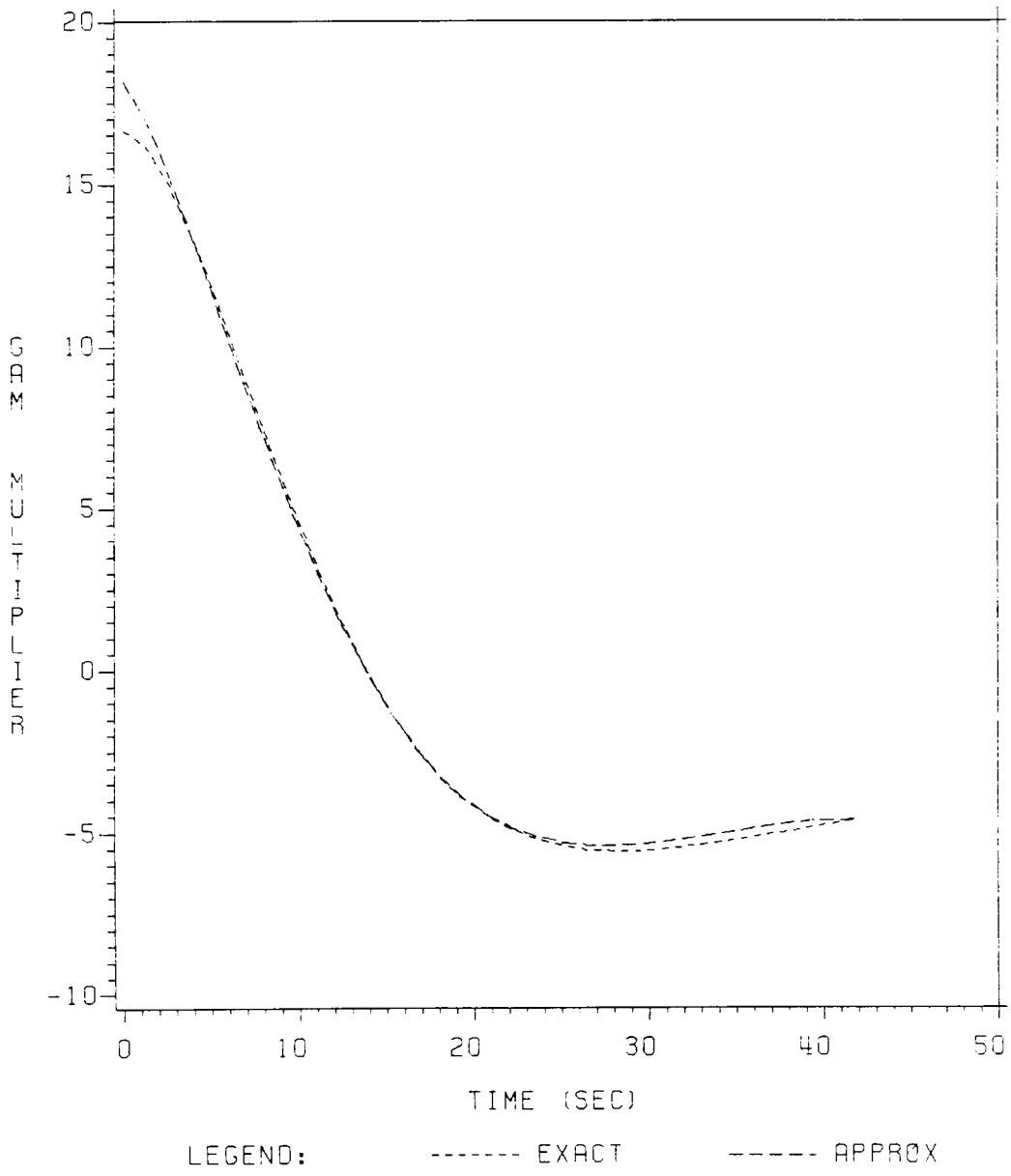

Figure 8. Comparison of γ-Multipliers (case B)
h_o=7 kft., γ_o=0.4 rad, E=200 kft.

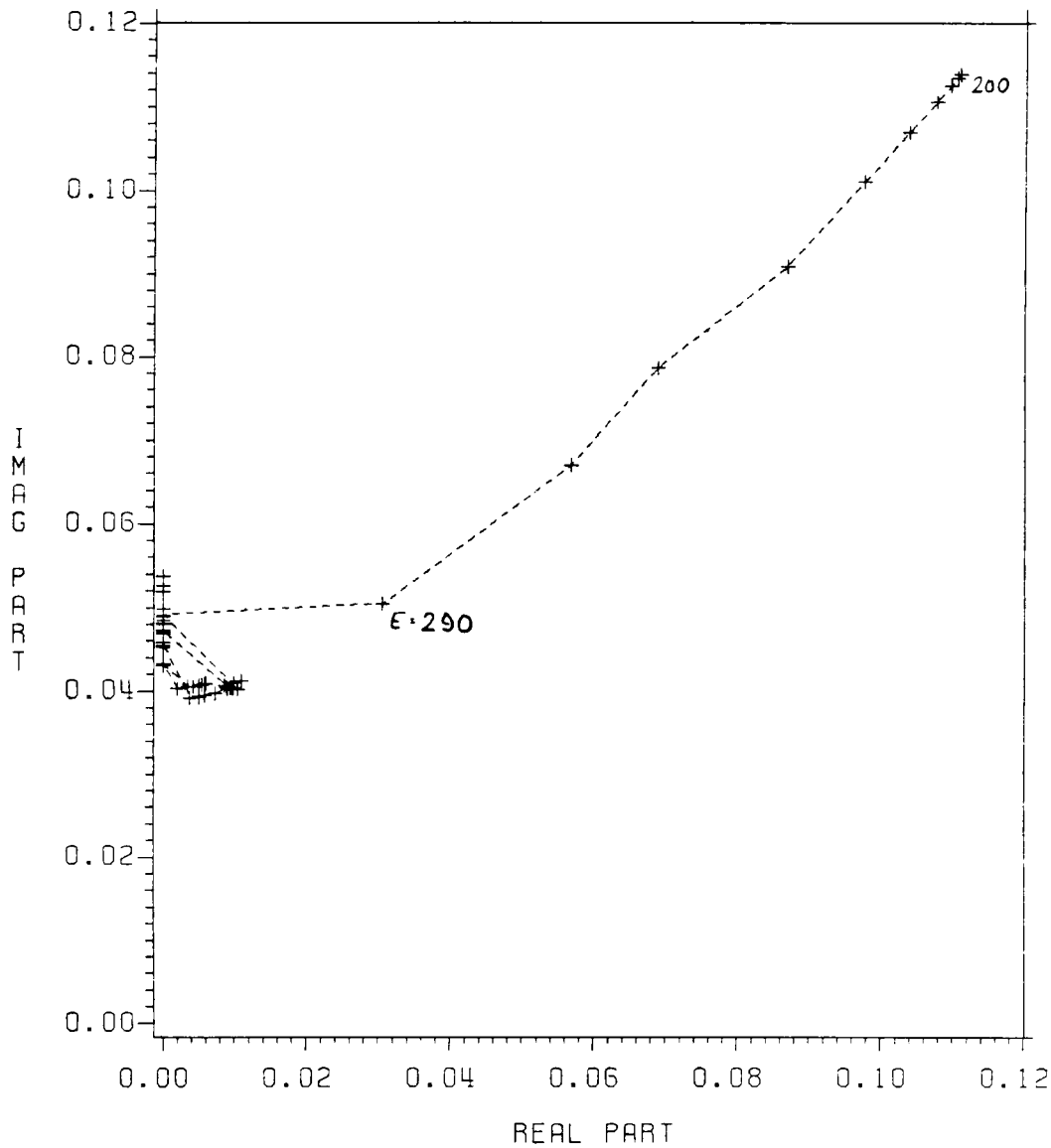

Figure 9. Locus of Roots as Function of Energy
E = 200 kft. to 690 kft. in 10 kft. steps

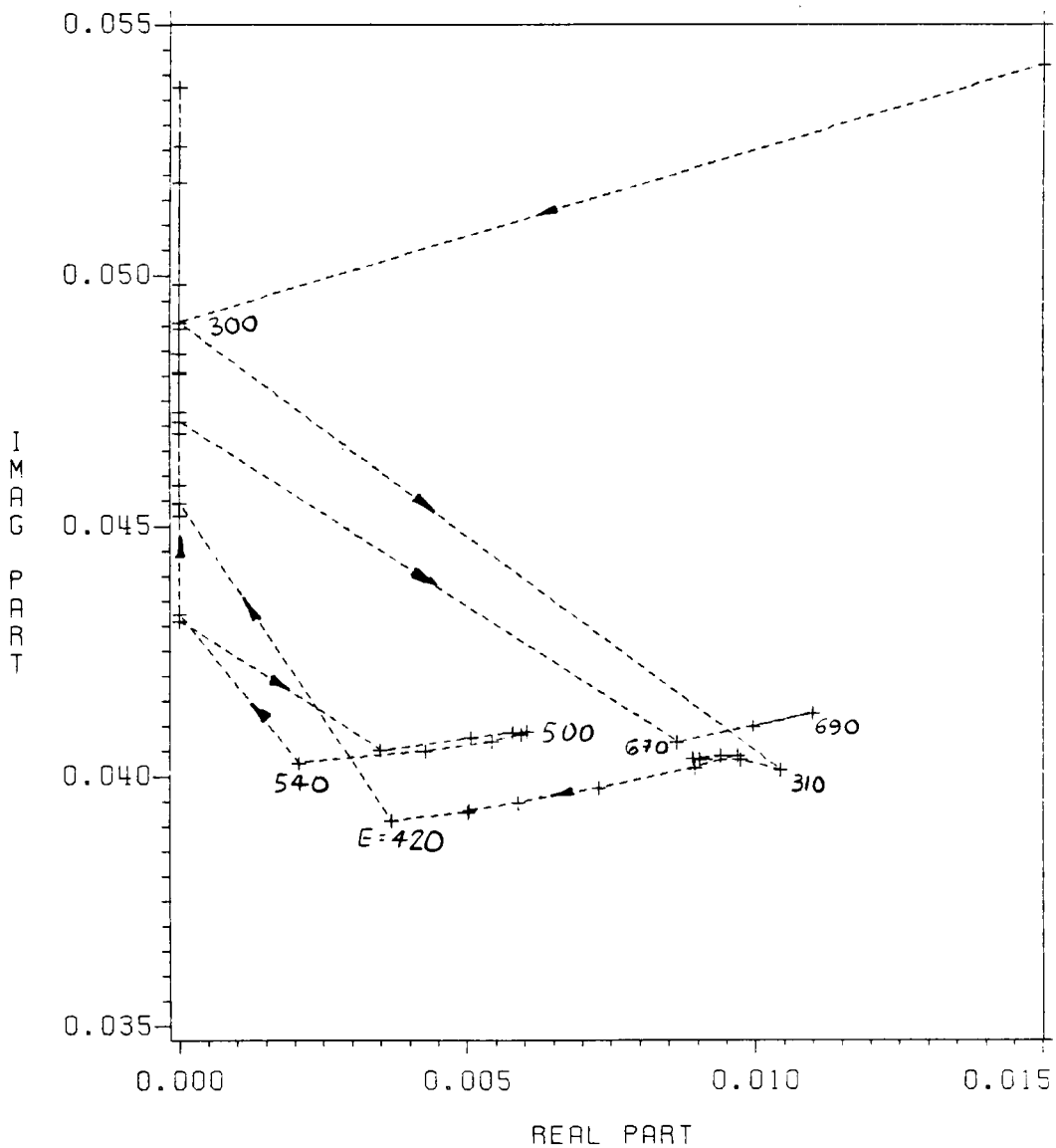

Figure 10. Detail of the Root-Locus
E = 300 kft. to 690 kft.

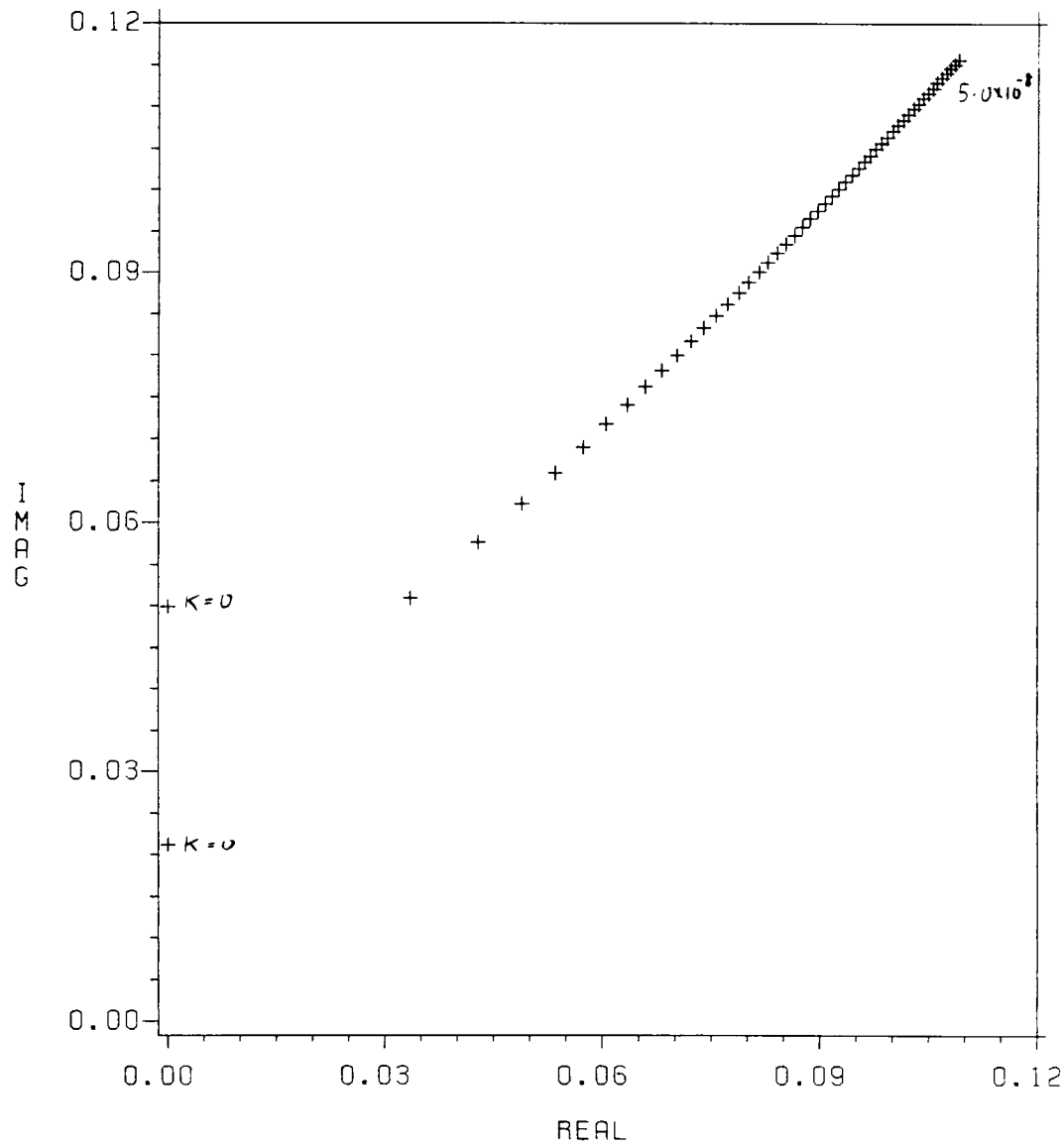

Figure 11. Root-Locus of Gain-Parameter K
E = 200 kft., K=0 to 5.0D-08 in steps of 1.d-09

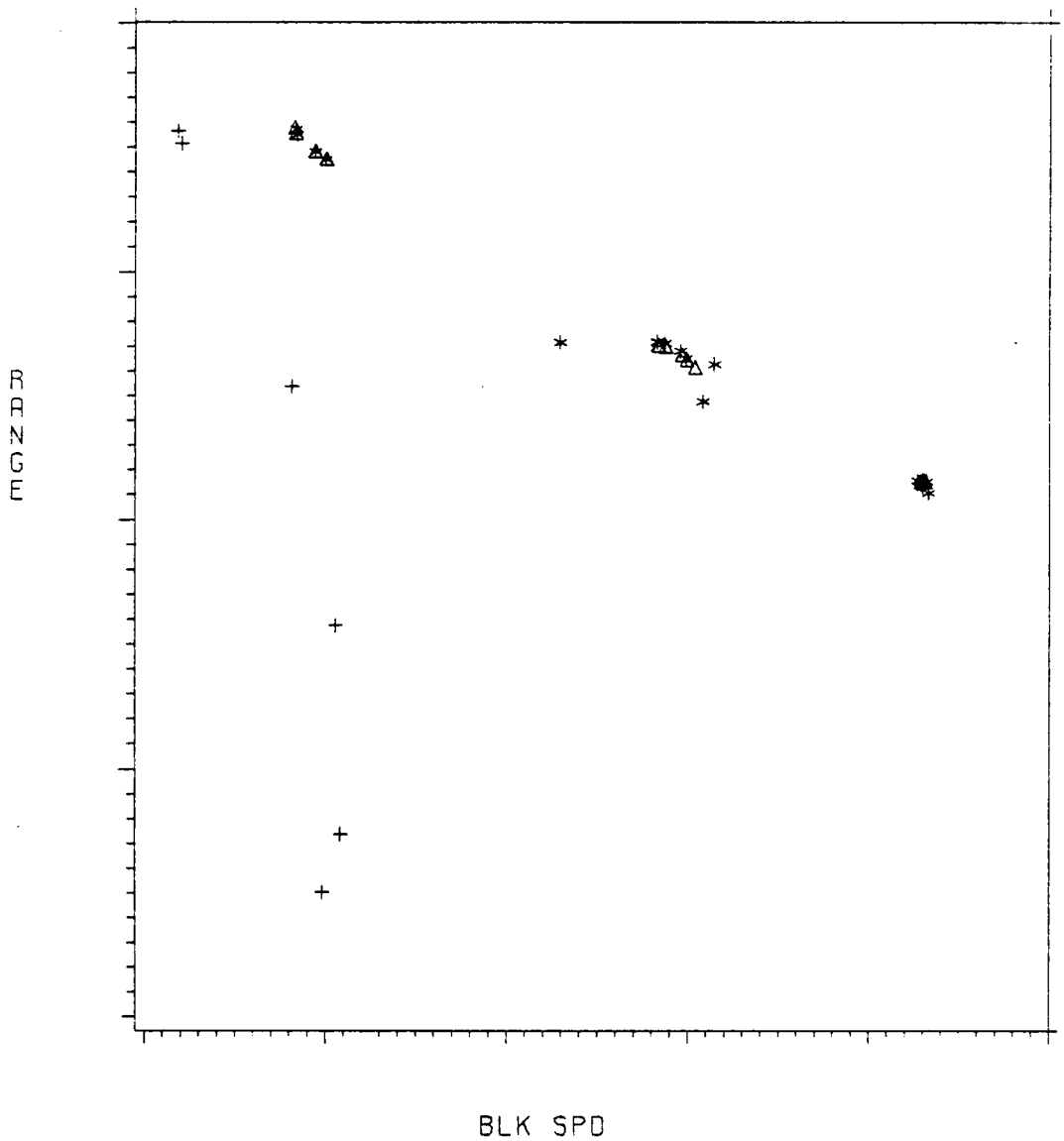

Figure 12. Range vs. Av.Speed, Full Trajectory Simulation
h_o=2.83Kft., γ_o=0.436rad, E_o=200Kft.

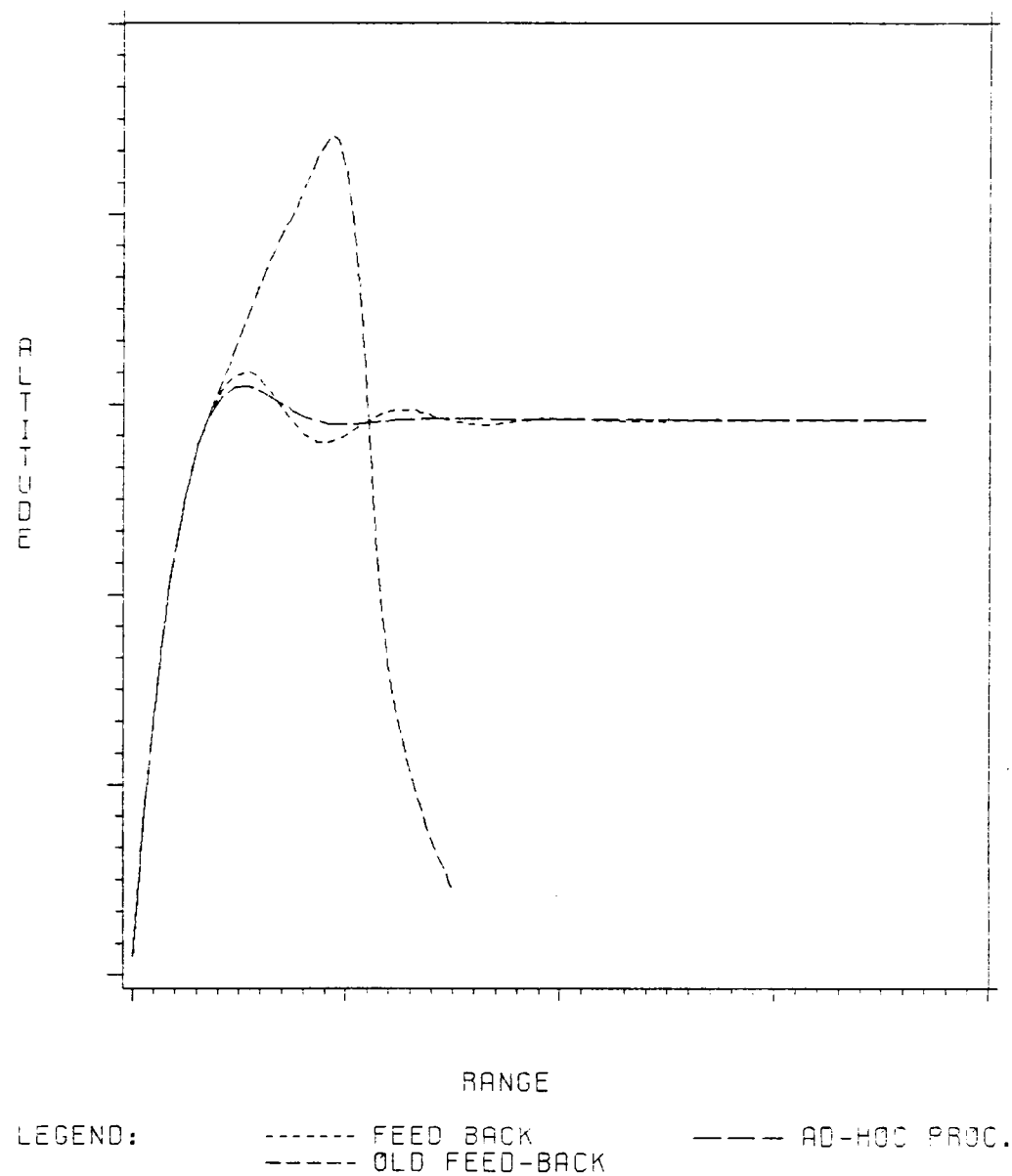

Figure 13. Altitude vs. Range, Full Trajectory Simulation

h_o=2.83Kft., γ_o=0.436rad, E_o=200Kft.

The vita has been removed from the scanned document